Title: The dorsal fan-shaped body is a neurochemically heterogeneous sleep-regulating center in *Drosophila*

Short Title: the dFB regulates sleep in *Drosophila*

Authors:

Joseph D. Jones[1#], Brandon L. Holder[1#], Andrew C. Montgomery[1], Chloe V. McAdams[1], Emily He[1], Anna E. Burns[1], Kiran R. Eiken[1], Alex Vogt[1], Adriana I. Velarde[1], Alexandra J. Elder[1], Jennifer A. McEllin[1] and Stephane Dissel[1*]

Affiliations:

[1]Division of Biological and Biomedical Systems, School of Science and Engineering, University of Missouri-Kansas City, Kansas City, Missouri, United States of America

co-first authors

[*]dissels@umkc.edu

Author contributions:

Conceptualization: SD

Methodology: SD, JDJ, BLH, ACM, JAM

Investigation: JDJ, BLH, ACM, CVM, EH, AEB, KRE, AV, AIV, AJE, JAM, SD

Visualization: JDJ, BLH, ACM, JAM, SD

Funding acquisition: SD

Project administration: SD

Supervision: SD

Writing – original draft: SD, JDJ, BLH, ACM, JAM

Abstract: Sleep is a behavior that is conserved throughout the animal kingdom. Yet, despite extensive studies in humans and animal models, the exact function or functions of sleep remain(s) unknown. A complicating factor in trying to elucidate the function of sleep is the complexity and multiplicity of neuronal circuits that are involved in sleep regulation. It is conceivable that distinct sleep-regulating circuits are only involved in specific aspects of sleep and may underlie different sleep functions. Thus, it would be beneficial to assess the contribution of individual circuits in sleep's putative functions. The intricacy of the mammalian brain makes this task extremely difficult. However, the fruit fly *Drosophila melanogaster,* with its simpler brain organization, available connectomics, and unparalleled genetics offers the opportunity to interrogate individual sleep-regulating centers. In *Drosophila*, neurons projecting to the dorsal Fan-Shaped Body (dFB) have been proposed to be key regulators of sleep, particularly sleep homeostasis. We recently demonstrated that the most widely used genetic tool to manipulate dFB neurons, the 23E10-GAL4 driver, expresses in two sleep-regulating neurons (VNC-SP neurons) located in the Ventral Nerve Cord (VNC), the fly analog of the vertebrate spinal cord. Since most data supporting a role for the dFB in sleep regulation have been obtained using 23E10-GAL4, it is unclear whether the sleep phenotypes reported in these studies are caused by dFB neurons or

VNC-SP cells. A recent publication replicated our finding that 23E10-GAL4 contains sleep-promoting neurons in the VNC. However, it also proposed that the dFB is not involved in sleep regulation at all. Unfortunately, this suggestion was made using genetic tools that are not dFB-specific. In this study, using a newly created dFB-specific genetic driver line, we demonstrate that the majority of 23E10-GAL4 dFB neurons can promote sleep when activated and that these neurons are involved in sleep homeostasis. In addition, we show that dFB neurons are neurochemically heterogeneous. Most dFB neurons express both glutamate and acetylcholine, while a minority of cells express only one of these two neurotransmitters. Importantly, dFB neurons do not express GABA, as previously suggested. Using neurotransmitter-specific dFB tools, our data also points at cholinergic dFB neurons as particularly potent at promoting sleep. Finally, we demonstrate that dFB-induced sleep can consolidate Short-Term Memory (STM) into Long-Term Memory (LTM), suggesting that the benefit of sleep on memory is not circuit-specific.

Introduction

Understanding the neural basis of behavior is a major aspect of neurobiology. However, unequivocally assigning a behavior to a specific neuron or group of neurons is not a trivial task. The extreme complexity, diversity, and connectivity of the mammalian nervous system renders this task even more daunting. To study the neural basis of a behavior, an investigator must be able to specifically manipulate a distinct group of cells and monitor the behavior of interest. Such approaches require precise genetic tools that allow for the manipulation of discrete neurons or groups of neurons. While such tools exist in mammalian systems (1), they may not be available for all the diverse types of cells that underlie a specific behavior. It is therefore not surprising

that animal models have been extensively used to untangle the neural basis of many different complex behaviors (2). One such model is the fruit fly *Drosophila melanogaster*, in which multiple binary systems have been developed to access and manipulate specific groups of neurons in the fly nervous system: GAL4/UAS (3), LexA/LexAop (4) and, QF/QUAS (5). Of these 3 systems, the GAL4/UAS system has been by far the most extensively used. However, the expression patterns of GAL4 drivers are often not restricted enough to clearly link a behavior to specific neurons. In such cases, refinement of GAL4 expression pattern can be achieved by employing the intersectional Split-GAL4 technology (6).

Sleep is a behavior that has been observed in a multitude of species ranging from jellyfish to humans (7). A priori, sleep could appear to be a detrimental activity as it competes with other motivated behaviors such as feeding, mating, or parenting, and renders organisms defenseless against potential predators. However, despite these negative outcomes, sleep has been maintained throughout evolution, emphasizing its essential value (8). Sleep is regulated by two processes, the circadian clock which gates the occurrence of sleep, and the sleep homeostat which controls the intensity and duration of sleep in response to prior wakefulness (9). Since the first characterization of sleep in *Drosophila* (10, 11), multiple studies have emphasized a high level of conservation of sleep mechanisms and regulation between flies and mammals (12). Like the mammalian system, sleep-regulating centers are found in many areas in the *Drosophila* brain (12, 13). Among them, neurons that project to the dorsal Fan-Shaped body (dFB) have attracted a lot of attention. Previous studies demonstrated that increasing the activity of neurons contained in the C5-GAL4, 104y-GAL4, and C205-GAL4 drivers strongly promotes sleep (14, 15). While the expression patterns of these 3 independent drivers are broad, they show prominent overlap in

the dFB (14). Based on these observations, the authors concluded that it is likely that the dFB plays a role in regulating sleep but could not rule out a role for neurons outside the dFB (14). In addition, further studies established that reducing the excitability of 104y-GAL4 neurons decreases sleep (16, 17). Highlighting the strong interaction between sleep and memory, activation of 104y-GAL4 neurons consolidates Short-Term Memory (STM) to Long-Term Memory (LTM) (14, 18) and restores STM to the classical memory mutants *rutabaga* and *dunce* (19). Further work supported a role for the dFB in sleep homeostasis by demonstrating that sleep deprivation increases the excitability of 104y-GAL4 dFB neurons (16). Taken together, these data pointed at 104y-GAL4 expressing neurons, probably dFB cells, as important modulators of sleep. However, it was demonstrated that 104y-GAL4 also expresses in neurons projecting to the ventral Fan-Shaped body (vFB) and that these neurons modulate sleep and are involved in the sleep dependent consolidation of STM into LTM (18), making the conclusions about the role of 104y-GAL4 dFB neurons uncertain. More recent studies using 23E10-GAL4, a more restrictive driver to manipulate and monitor dFB neurons (20, 21), proposed that increasing sleep pressure switches dFB neurons from an electrically silent to an electrically active state, and that this process is regulated by dopaminergic signaling to the dFB (20) and the accumulation of mitochondrial reactive oxygen species in dFB neurons (22). Because of their physiological properties, dFB neurons have been proposed to be the fly functional analog to the ventrolateral preoptic nucleus (VLPO), a key center regulating sleep homeostasis in the mammalian brain (16, 23).

Chronic and acute activation (using thermogenetic or optogenetic methods) of 23E10-GAL4 neurons increases sleep (18, 24-28). Since it has a relatively restricted expression pattern and a

strong capacity to modulate sleep, 23E10-GAL4 (as it relates to sleep) is seen as a dFB specific driver by most in the scientific community. However, our recent work, aimed at identifying individual sleep-regulating 23E10-GAL4 expressing neurons, demonstrated that this driver is not as dFB-specific as previously believed. In particular, we demonstrated that 23E10-GAL4 expresses in two cholinergic sleep-promoting cells (VNC-SP neurons) located in the Ventral Nerve Cord (VNC) (27). Additional work from another laboratory confirmed that there are VNC-localized sleep-promoting neurons in the 23E10-GAL4 driver (28). Together, these findings have raised some serious questions about the role, if any, of the dFB in sleep regulation, especially if these data were obtained using 23E10-GAL4. In fact, a recent study suggests that the dFB has no sleep-regulating capacity (28). However, the conclusions made by these authors are based on data obtained with non-specific tools. In this study, we sought to unequivocally assess the role of the dFB in sleep regulation by conducting a targeted, intersectional Split-GAL4 screen (6) focused on 23E10-GAL4 dFB neurons. We report here that sleep-promoting VNC-SP neurons are present in most Split-GAL4 lines we created, making it difficult to assess the role of the dFB using these lines. However, we identified a dFB-specific Split-GAL4 line that can be used to manipulate most 23E10-GAL4 dFB neurons. Using this novel driver, we demonstrate that 23E10-GAL4 dFB cells regulate sleep, especially sleep homeostasis, and that this dFB-induced sleep promotes the consolidation of STM to LTM. In addition, our work reveals that dFB neurons are neurochemically heterogeneous and that cholinergic dFB neurons play an important role in sleep promotion.

Results

A dFB-based Split-GAL4 screen identifies multiple sleep-promoting lines

To assess the role of 23E10-GAL4 dFB neurons in sleep regulation, we designed a Split-GAL4 screen (6) focused on the dFB. The Split-GAL4 technology separates the functional GAL4 transcription factor into two non-functional fragments, a GAL4 DNA-binding domain (DBD) and an activation domain (AD). Expression of the AD and DBD fragments is controlled by different enhancers and the functional GAL4 transcription factor is reconstituted only in the cells in which both fragments are expressed (6). We obtained 20 different AD lines based on their associated GAL4 line expressing in the dFB, as observed using the Janelia Flylight website (21, 29). Since the goal of our screen was to identify the contribution of 23E10-GAL4 dFB neurons in sleep regulation, we designed a targeted approach by combining these individual AD lines to a 23E10-DBD line (29, 30), thus creating 20 new Split-GAL4 lines named FBS for Fan-Shaped Body Splits (See S1 Table for a description of these lines). These newly created lines were screened behaviorally for their ability to modulate sleep and anatomically to identify their expression patterns. To do so, each individual Split-GAL4 FBS line was crossed to 1) a line expressing both the thermogenetic TrpA1 cation channel (31) and a mCD8GFP construct and 2) the optogenetic CsChrimson actuator (32).

For the thermogenetic screen, flies were maintained at 22°C for 2 days before raising the temperature to 31°C at the beginning of day 3 for a duration of 24h. Temperature was brought down to 22°C on day 4 (Fig 1A). For each individual fly, we calculated the percentage of total sleep change between activation day (day3) and baseline day (day2) (Fig 1A). As a control for this screen, we used an enhancerless AD construct (created in the vector used to make all the AD lines) combined with 23E10-DBD, since it is the common element in all the Split-GAL4 lines analyzed in this screen. As seen in Fig 1B, acute thermogenetic activation of the neurons

contained in 4 of the 20 FBS lines led to significant increases in sleep in female flies (FBS42, FBS45, FBS53, FBS68), when compared with controls. Individual sleep traces for these 4 lines are shown in Fig 1D-1H. Sleep profiles of the other 16 FBS lines are shown in S1 Fig. Importantly, analysis of activity counts during awake time reveals that increases in sleep are not caused by a reduction in locomotor activity (S2A Fig), ruling out motor deficits or paralysis. On the contrary, 2 of the sleep-inducing lines even showed an increase in waking activity upon neuronal activation. This increase is likely explained by the need for a fly to perform tasks that are mutually exclusive to sleep in a reduced amount of waking time. While increases in total sleep are indicative of increased sleep quantity, this measurement does not provide information about sleep quality or sleep depth. Previous work proposed that increased sleep bout duration is an indication of increased sleep depth (33). To assess whether sleep quality is modulated when activating FBS lines, we analyzed sleep consolidation during the day and night in these flies. As seen in S2B Fig, daytime sleep bout duration is significantly increased upon thermogenetic activation in 7 out of 20 FBS lines (FBS28, FBS42, FBS45, FBS53, FBS68, FBS72 and FBS84). Interestingly, of those 7 lines, 3 did not show an increase in total sleep (FBS28, FBS72 and FBS84). During the nighttime, the effect of high temperature on sleep is obvious as most lines, including the control, display a significant decrease in sleep bout duration when raising the temperature to 31°C (S2C Fig). These data agree with previous studies documenting that changes in temperature modulate sleep architecture and that high temperature disturbs sleep at night (34-37) . Only 4 of the 20 FBS lines (FBS42, FBS45, FBS53 and FBS68) maintain similar nighttime sleep bout durations before and during thermogenetic activation. Importantly, in 3 of these 4 lines, nighttime sleep bout duration is significantly increased at 31°C when compared to control flies (S2C Fig).

Since sleep in *Drosophila* is sexually dimorphic (38-40), we systematically assessed male flies in our experiments. As seen in S3A Fig, thermogenetic activation increases total sleep in males using 7 out of the 20 FBS lines, including the 4 lines that increase total sleep in females (FBS42, FBS45, FBS53, FBS68, FBS72, FBS81 and FBS84). These effects on total sleep are not caused by motor deficits or paralysis as waking activity is not reduced in long sleeping male flies (S3B Fig). Daytime sleep bout duration is significantly increased in 6 out of these 7 lines (S3C Fig). When examining nighttime sleep, thermogenetic activation of FBS45 and FBS68 significantly increases bout duration while FBS42, FBS53, FBS81 and FBS84 show no difference between 22°C and 31°C (S3D Fig). Altogether, our thermogenetic approach identified 8 FBS lines that increase total sleep and/or sleep bout duration when activated (S2 Table).

Because of the strong effect that temperature has on sleep, we sought to confirm our thermogenetic findings using an alternative method to manipulate FBS lines. The logic behind our thinking is that it may be difficult to fully describe and characterize the sleep behaviors of our FBS lines when temperature itself has such a profound effect on sleep. Furthermore, a recent study demonstrated that some of the effects of high temperature on sleep are mediated by GABAergic transmission on dFB neurons (37). We thus undertook an optogenetic screen using CsChrimson (32). Our optogenetic experimental setup is described in Fig 1A. Notably, for neurons to be activated when expressing CsChrimson, flies need to be fed all trans-retinal and the neurons must be stimulated with a 627nm LED light source (32). Thus, optogenetic approaches provide a much better control on the timing and parameters of activation. Our optogenetic activation screen gave results that are mostly identical to the thermogenetic approach. That is, all 4 sleep-promoting lines identified using TrpA1 also increase total sleep

when activated with CsChrimson in retinal-fed female flies (FBS42, FBS45, FBS53 and FBS68) (Fig 1C). Interestingly, activation of neurons contained in FBS70 and FBS72 is sleep-promoting in retinal-fed female flies while it was not using TrpA1 (Fig 1B and 1C). Looking at males, optogenetic activation increases total sleep in all 7 sleep-promoting lines identified using TrpA1 (FBS42, FBS45, FBS53, FBS68, FBS72, FBS81 and FBS84) as well as an 8th line (FBS33) (S4A Fig). Importantly, these optogenetic sleep-promoting effects are not the result of locomotor deficits (S4B Fig for males and S5A Fig for females).

Examination of sleep bout duration in retinal-fed flies indicates that most sleep-promoting FBS lines increase sleep consolidation during the day (S4C Fig for males and S5B Fig for females) and during the night (S4D Fig for males and S5C Fig for females). Interestingly, some FBS lines that did not increase total sleep upon optogenetic activation increased daytime sleep bout duration: FBS57, FBS60, FBS81 and FBS84 in females (S5B Fig) and FBS35, FBS64 and FBS87 in males (S4C Fig). In addition, optogenetic activation of neurons contained within FBS58 increases nighttime sleep bout duration in females (S5C Fig). These data suggest that these lines may also express in sleep-regulating neurons. Importantly, analysis of sleep parameters in vehicle-fed flies demonstrate that the sleep phenotypes we observed are specific to retinal-fed and LED stimulated flies (S6 Fig for females and S7 Fig for males).

A summary of sleep-modulating effects for all FBS lines in both activation protocols is provided in S2 Table. Taken together, our thermogenetic and optogenetic screens revealed that activating neurons contained within 16 FBS lines increases at least one sleep parameter. Among these 16 lines, 7 are consistently increasing total sleep and sleep consolidation in females and males using

both activation protocols (FBS42, FBS45, FBS53, FBS68, FBS72, FBS81, and FBS84) (S2 Table).

VNC-SP neurons are present in most FBS lines

Having identified 16 different Split-GAL4 lines that significantly increase at least one sleep parameter when thermogenetically or optogenetically activated, we sought to identify the neurons that are contained within these lines. As seen in Fig 1D-1H and S1 Fig, 19 out of 20 lines express in dFB neurons, with only FBS25 showing no expression at all in the brain and VNC. Since FBS25 expresses in no neurons at all, it is not surprising that no sleep changes were seen using both activation protocols, as FBS25 should behave like a control. The number of dFB neurons contained within different FBS lines ranges from 4 to 27 per brain on average (S1 Table). Most lines show very little additional expression in the brain and there is no consistency in these additionally labeled cells between different lines. However, 18 out of the 19 lines that express in dFB neurons also express in cells in the metathoracic ganglion of the VNC. This is not surprising as our previous study showed that the 23E10-GAL4 driver, on which this Split-GAL4 screen is based, expresses in 4 neurons located in the metathoracic ganglion of the VNC, 2 TPN1 neurons (41) and the two VNC-SP cells (27). Most FBS lines (17) express in neurons that have similar anatomical features as VNC-SP neurons in the VNC and in the brain, displaying very typical processes that we previously named “bowtie” (27). These “bowtie” processes are located extremely close to the axonal projections of dFB neurons, making their visualization sometimes difficult, depending on the strength of dFB projections’ staining. Importantly, all 16 FBS lines that increase at least one sleep parameter when activated express in these VNC-SP-like cells, in

addition to dFB neurons. Furthermore, most FBS lines (14) also express in cells that appear to be TPN1 neurons (41).

Our previous study demonstrated that VNC-SP neurons are cholinergic and that the expression of the Split-GAL4 repressor KZip^{+} (42) under the control of a ChAT-LexA driver effectively blocks the accumulation of reconstituted GAL4 in VNC-SP neurons (27). Since we observed neurons reminiscent of VNC-SP in all 4 FBS lines that increase sleep when thermogenetically activated in females, we wondered whether VNC-SP neurons are the cells responsible for the sleep increase in these lines. To address this possibility, we expressed TrpA1 and GFP in FBS42, FBS45, FBS53, and FBS68 neurons while simultaneously driving the expression of the KZip^{+} repressor in ChAT-LexA cells. As seen in S8A-S8D Fig, expressing the KZip^{+} repressor in cholinergic cells abolishes GFP expression in the metathoracic ganglion in all *FBS>UAS-GFP; ChAT-LexA>LexAop2-KZip*$^{+}$ flies. These data demonstrate that VNC-SP neurons are present in the expression pattern of all 4 FBS lines tested. When assessing sleep, expressing the KZip^{+} repressor in ChAT-LexA cells prevents the increase in sleep seen in all *FBS>UAS-TrpA1* flies tested (S8E Fig). These data suggest that the neurons responsible for the sleep increase observed when thermogenetically activating FBS42, FBS45, FBS53, and FBS68 cells are the cholinergic VNC-SP neurons. However, since we previously demonstrated that some 23E10-GAL4 dFB neurons are cholinergic (27), it is possible that cholinergic 23E10-GAL4 dFB neurons may also participate in these sleep phenotypes. Based on these data, and our previous work showing that 23E10-GAL4 expresses in VNC-SP cells (27), we believe that all 16 FBS sleep-promoting lines express in VNC-SP neurons, making it impossible for us to assess whether 23E10-GAL4 dFB neurons modulate sleep using these lines.

However, if VNC-SP neurons are present in most FBS lines, why do not we see any sleep changes with one of them (FBS1)? In addition, why are some VNC-SP expressing FBS lines more potent than others at promoting sleep? We hypothesized that these differences may be explained by different strength of expression of the reconstituted GAL4 in VNC-SP neurons in FBS lines. To address this, we decided to use a GFP-DD construct which is normally degraded by the proteasome (43). Degradation is blocked when feeding the flies trimethoprim (TMP) (43) and expression levels can be assessed. As controls, we used 23E10-GAL4 and the VNC-SP Split-GAL4 line previously described (27). Flies were maintained on standard food until they reached 5-6 days of age. Then half of the flies were fed either vehicle control (DMSO) or TMP, to protect GFP-DD from degradation, for 24h (S9A Fig). Flies were then dissected and GFP levels were measured in the metathoracic ganglion of the VNC. As seen in S9B and S9C Fig, feeding TMP leads to strong increases in GFP signal in VNC-SP neurons when GFP-DD is expressed using 23E10-GAL4, VNC-SP Split, and FBS45. When GFP-DD is expressed in FBS33 cells, we observed a moderate increase in GFP signal intensity. Finally, with two lines, FBS1 and FBS58, we saw no statistical differences between DMSO-fed and TMP-fed flies. The strength of expression in VNC-SP neurons correlates well with the magnitude of sleep increases seen when activating the different lines (S2 Table). FBS45 is strongly sleep-promoting when thermogenetically and optogenetically activated, while FBS33 only increases total sleep and daytime sleep bout duration in males using optogenetic activation. Finally, FBS58 has a very modest impact on sleep while FBS1 has none. Thus, we conclude that within our FBS lines, the strength of expression in VNC-SP neurons dictates how potently a given line can modulate sleep.

When combining behavioral and anatomical data, we conclude that the numbers of dFB neurons contained within a specific FBS line cannot be predictive of whether the line can strongly promote sleep upon neuronal activation. For example, FBS68 strongly increases all sleep parameters in both sexes and activation protocol while only expressing in 3-6 dFB neurons (Fig 1H, S1 and S2 Tables). On the other hand, FBS60 contains 22-27 dFB neurons and only increases daytime sleep bout duration in females using optogenetic activation (S1J Fig, S1 and S2 Tables). The anatomical feature that is predictive of whether a FBS line can modulate sleep or not is the presence/absence of VNC-SP neurons within the pattern of expression. In addition, how strongly a line expresses in VNC-SP neurons dictates how strongly sleep-promoting that line is (S9B and S9C Fig).

In conclusion, our activation screens and anatomical analysis identified 16 sleep-promoting FBS lines expressing in diverse numbers of dFB neurons. However, all 16 lines contain the previously identified sleep-promoting VNC-SP neurons. Thus, these lines are not well suited to unequivocally assess the role of 23E10-GAL4 dFB neurons in sleep.

Identification of a dFB-specific Split-GAL4 line

In our screen, we only identified two FBS lines that express in dFB neurons but not in VNC-SP cells (FBS6 and FBS41). No sleep parameters are increased when activating neurons contained within both lines. However, both lines only express in a reduced number of dFB neurons (S1 Fig and S1 Table). Thus, these two lines are not fully recapitulating the dFB expression pattern of the 23E10-GAL4 driver. Fortunately, we identified an additional FBS line (84C10-AD; 23E10-DBD which we named dFB-Split) that expresses in 18-27 dFB neurons per brain and no other cells in

the brain or VNC (Fig 2A, S1 and S2 Movies, S1 Table). Since we previously reported that 23E10-GAL4 reliably labels 23-30 dFB neurons in our confocal microscopy experiments (27), we conclude that dFB-Split expresses in 78-90% of 23E10-GAL4 dFB neurons. Additionally, dFB-Split does not express in the wings, legs, gut, and ovaries (S10 Fig). Though not being a complete replication of all 23E10-GAL4 dFB neurons, we hypothesized that the dFB-Split line is a good tool to assess a role for 23E10-GAL4 dFB neurons in sleep regulation. For clarity, we will refer to the dFB cells contained in the dFB-Split expression pattern as $dFB^{23E10\cap 84C10}$ neurons.

Activation of $dFB^{23E10\cap 84C10}$ neurons promotes sleep

Having identified a genetic driver that is dFB-specific and includes the majority of the 23E10-GAL4 dFB neurons, we sought to investigate the contribution of these cells to sleep. Using our standard optogenetic protocol, we find no sleep increases when activating $dFB^{23E10\cap 84C10}$ neurons in females and males (Fig 2B-2D). Note that this activation protocol is sufficient to increase sleep using multiple other drivers (Fig 1C) and the VNC-SP Split-GAL4 (27) indicating that it is effective at activating neurons. Why, then, does this protocol not cause an effect in $dFB^{23E10\cap 84C10}$ neurons? Previous studies have demonstrated that the dFB is under strong dopaminergic inhibition (15, 17, 20, 44) and that dopamine is a key factor regulating whether dFB neurons are active or silent (20). In addition, it was shown that sleep deprivation increases the activity of dFB neurons, switching them to the active state (16). We hypothesize that in our experiments, sleep pressure is low as flies are allowed to sleep normally before activation. Thus, the inhibitory activity of dopaminergic inputs to the dFB should be relatively strong and it is possible that our standard activation protocol may not be sufficient to overcome this inhibition.

To test this possibility, we decided to increase the intensity of our optogenetic activation protocol. As seen in Fig 2E and 2F, a 20Hz activation protocol increases total sleep in females. In addition, it significantly increases daytime and nighttime sleep bout duration (S11B Fig and S11C Fig). These effects are not due to a locomotor deficit as waking activity is unaffected by a 20Hz activation in females (S11A Fig). Importantly, these increases in daytime and nighttime sleep consolidation are not seen in vehicle-fed flies (S11E and S11F Fig). We found similar sleep promoting effects when looking at *dFB-Split>CsChrimson* males subjected to a 20Hz optogenetic activation (Fig 2G and S11G-S11L Fig).

We next used a 50Hz activation protocol. As seen in Fig 2H-2J, total sleep is increased in *dFB-Split>CsChrimson* females and males when activated with a 50Hz protocol. Furthermore, daytime and nighttime sleep bout durations are increased in females using this activation protocol (S12B and S12C Fig). Again, these effects are not the result of abnormal locomotor activity (S12A Fig for females and S12G Fig for males) and are not seen in vehicle-fed flies (S12E and S12F Fig).

To further validate that optogenetic activation of $dFB^{23E10\cap 84C10}$ neurons increases sleep, and not any other behavior (feeding, grooming, or in-place micromovements) that could be falsely registered as sleep by the single beam DAM2 system, we employed the more sensitive multibeam activity monitors (DAM5H, Trikinetics) that contain 15 independent infrared beams, separated by 3 mm across the tube length. As seen in Fig 2K, a 50 Hz optogenetic activation significantly increases sleep in *dFB-Split>CsChrimson* females as assessed using the DAM5H multibeam system, ruling out the possibility that we misregistered micromovements as sleep.

Since our data suggested a direct relationship between the intensity of the optogenetic activation protocol and the capacity of dFB$^{23E10\cap 84C10}$ neurons to increase sleep, we decided to try to turn the 627nm LEDs on constantly. As seen in Fig 2L, constant LED activation of dFB$^{23E10\cap 84C10}$ neurons significantly increase sleep confirming that there is a direct relationship between strength of activation and sleep increase. We also performed video analysis of multiple behaviors before and during constant optogenetic activation of dFB$^{23E10\cap 84C10}$ neurons and we found that times spent feeding, grooming, and walking are significantly reduced in *dFB-Split>CsChrimson* flies during activation while time spent sleeping is significantly increased (Fig 2M).

Finally, we investigated whether activation of dFB$^{23E10\cap 84C10}$ neurons modulate arousal threshold by applying mechanical stimulations of increasing strength to *dFB-Split>CsChrimson* flies. As seen in Fig 2N, when dFB$^{23E10\cap 84C10}$ neurons are activated (retinal-fed, LED ON), a significantly lower percentage of flies are awakened by the 20% and 40% stimulus strength, compared with non-activated flies (retinal-fed, LED OFF). Importantly, at the higher stimuli strength (60%, 80% and 100%), there are no differences between activated and non-activated *dFB-Split>CsChrimson* flies, indicating that these flies can respond to a stimulus that is strong enough (i.e., these flies are not paralyzed). These data suggest that activation of dFB$^{23E10\cap 84C10}$ neurons increases arousal threshold, an indicator of sleep depth.

Thus, we conclude that activation of dFB$^{23E10\cap 84C10}$ neurons can increase sleep and sleep depth.

Silencing dFB$^{23E10\cap 84C10}$ neurons increases sleep and reduces sleep homeostasis

After demonstrating that activation of dFB$^{23E10\cap 84C10}$ neurons increases sleep duration and sleep depth, we performed experiments to silence the activity of these neurons chronically by expressing the hyperpolarizing inward rectifying potassium channel Kir2.1 (45). First, we

assessed whether the constitutive expression of Kir2.1 in dFB$^{23E10\cap 84C10}$ neurons leads to anatomical defects. As seen in S13A and S13B Fig, we observed no defects in dFB$^{23E10\cap 84C10}$ neuron numbers or processes when expressing Kir2.1, compared with controls. Surprisingly, total sleep is significantly increased when expressing Kir2.1 in dFB$^{23E10\cap 84C10}$ neurons in female flies (Fig 3A and 3B). This effect on sleep is accompanied by an increase of daytime sleep bout duration (Fig 3D) while consolidation at night is unchanged (Fig 3E). These enhancements on sleep are not due to locomotor deficits (Fig 3C). We obtained identical behavioral results when expressing Kir2.1 in dFB$^{23E10\cap 84C10}$ neurons of male flies (S13C-S13F Fig). These results are somewhat surprising as they are similar to the ones obtained when activating dFB$^{23E10\cap 84C10}$ neurons. We thus decided to investigate them further. First, we repeated these behavioral experiments using the multibeam system. As seen in Fig 3F, hyperpolarization of dFB$^{23E10\cap 84C10}$ neurons increases total sleep as assessed with DAM5H monitors. Thus, chronic hyperpolarization of dFB$^{23E10\cap 84C10}$ neurons increases sleep and sleep consolidation without disrupting the anatomical properties of these cells. To further investigate the effects of silencing dFB$^{23E10\cap 84C10}$ neurons, we employed an acute silencing approach by expressing Shi^{ts1} (46). Acute silencing (24h, Fig 3G) of dFB$^{23E10\cap 84C10}$ neurons has no effect on sleep in females (Fig 3H) or males (Fig 3I). Altogether, our silencing data further demonstrate that dFB$^{23E10\cap 84C10}$ neurons regulate sleep. However, further work is needed to explain why both activation and chronic silencing lead to sleep increases.

Multiple studies have suggested a role for dFB neurons in regulating sleep homeostasis. In particular, sleep deprivation increases the excitability of dFB neurons (16) and augmented sleep pressure switches dFB neurons from an electrically silent to an electrically active state (20).

Furthermore, reducing the excitability of dFB neurons by reducing levels of the Rho-GTPase-activating protein encoded by the crossveinless-c (cv-c) gene leads to a defect in sleep homeostasis (16). We previously demonstrated that hyperpolarizing all 23E10-GAL4 neurons blocks sleep homeostasis, however this effect was not due to VNC-SP neurons (27). Thus, we concluded that there must be 23E10-GAL4 expressing neurons that are not VNC-SP cells that are involved in sleep homeostasis. Could these neurons be dFB$^{23E10\cap 84C10}$ cells? To test this possibility, we expressed Kir2.1 in dFB$^{23E10\cap 84C10}$ neurons, subjected flies to 12h of mechanical sleep deprivation (SD) during the night and monitored recovery sleep for the subsequent 48h. We observed that control flies show a gradual recovery of lost sleep over the 48h period (Fig 3J). Hyperpolarizing dFB$^{23E10\cap 84C10}$ neurons led to an interesting pattern as *dFB-Split>Kir2.1* flies show some recovery during the first 4-6h following SD, but then did not show additional gains during the remaining recovery period (Fig 3J). To further demonstrate our finding, we quantified sleep recovery after 4h, 6h, 12h, 24h, and 48h. As seen in Fig 3K, sleep recovery is significantly reduced between controls and *dFB-Split>Kir2.1* flies at all time points. However, in *dFB-Split>Kir2.1* flies, sleep recovery at 4h, 6h, 12h, and 24h is significantly different from 0, indicating that these flies show a weaker, but not non-existent, homeostatic rebound (Fig 3K). These data suggest that hyperpolarizing dFB$^{23E10\cap 84C10}$ neurons does not fully block sleep homeostasis, especially in the immediate period following sleep-deprivation. Interestingly, another work showed that hyperpolarizing all 23E10-GAL4 neurons does not impair early (6h) sleep homeostasis (28). In conclusion, our data suggests that there may be multiple groups of neurons involved in sleep homeostasis in the fly brain, with dFB$^{23E10\cap 84C10}$ neurons being an important, but not the sole, player.

dFB$^{23E10\cap 84C10}$ neurons express acetylcholine and glutamate

Previous studies have proposed that dFB neurons are GABAergic (47, 48). However, since these data were obtained using a driver that is not dFB-specific (27), the neurochemical identity of dFB neurons is uncertain. In addition, we showed in our previous work (27) that some 23E10-GAL4 dFB neurons are cholinergic. We thus investigated whether dFB neurons are GABAergic, glutamatergic, or cholinergic by expressing GFP in dFB$^{23E10\cap 84C10}$ neurons and staining them with antibodies to GABA, choline acetyltransferase (ChAT), the enzyme necessary to produce Acetylcholine, and the vesicular glutamate transporter (VGlut). As seen in Fig 4A, we observed no GABA staining in dFB$^{23E10\cap 84C10}$ neurons, but we found that a minority of these cells express ChAT only or VGlut only, while more than 50% of them express both neurotransmitters (Fig 4B and 4C). To confirm our findings, we employed a Split-GAL4 strategy using the 84C10 component of dFB-Split paired with neurotransmitter-specific Split elements. As seen in Fig 4D and 4G, an 84C10-AD; Gad1-DBD Split-GAL4 line shows no expression at all in the brain, VNC, and dFB. An 84C10-AD; ChAT-DBD line expresses in about 16 dFB neurons (named dFB$^{ChAT\cap 84C10}$) per brain and no other cells in the brain and VNC (Fig 4E and 4G, S3 and S4 Movies). Finally, a VGlut-AD; 84C10-DBD expresses in 22 dFB cells (named dFB$^{VGlut\cap 84C10}$) per brain and shows no other expression in the brain and VNC (Fig 4F and 4G, S5 and S6 Movies). Note that while this manuscript was in preparation, a preprint reported that dFB neurons are glutamatergic (49). Taken together, our immunostaining data and Split-GAL4 approach indicate that dFB$^{23E10\cap 84C10}$ neurons are not homogenous when it comes to neurochemical identity and can be divided in 3 categories. Most dFB$^{23E10\cap 84C10}$ neurons express both ChAT and VGlut (ChAT^{+}, VGlut^{+} cells), while others express only VGlut (ChAT^{-}, VGlut^{+} cells) or ChAT (ChAT^{+}, VGlut^{-} cells). Given that acetylcholine is the main excitatory

neurotransmitter in the fly system and that glutamate is inhibitory in dFB neurons (49), it is fair to expect that these 3 categories of dFB$^{23E10\cap 84C10}$ neurons may differentially affect sleep.

To investigate this possibility, we employed optogenetic activation (Fig 4H-4J). A 50Hz optogenetic activation of dFB$^{ChAT\cap 84C10}$ neurons strongly increases total sleep while it does not when dFB$^{VGlut\cap 84C10}$ neurons are activated (Fig 4J and 4K). The increase in sleep when activating dFB$^{ChAT\cap 84C10}$ neurons is not caused by a general deficit in locomotor activity. In fact, when LED activated *dFB$^{ChAT\cap 84C10}$>CsChrimson* flies are awake, they move more than unactivated controls (Fig 4M). While it does not increase total sleep, activation of the glutamatergic population of dFB neurons increase daytime sleep (Fig 4I and 4L) but significantly less than activation of the cholinergic neurons (Fig 4L). These data suggest that within the heterogeneous dFB population, cholinergic neurons play a major role in the sleep-promoting capacity of this region.

The sleep induced by dFB$^{23E10\cap 84C10}$ neuronal activation consolidates STM to LTM

The relationship between sleep and memory is well documented (13, 50, 51). In particular, sleep plays a role in the consolidation of STM into LTM (52). Employing genetic and pharmacological activation, previous studies have demonstrated that inducing sleep after a courtship memory training protocol that is sufficient to create STM but not LTM, could convert that STM to LTM in *Drosophila* (14, 18, 19). Sleep depriving flies while sleep-promoting neurons were activated abrogated the formation of LTM, demonstrating that sleep was needed for this effect (14). More recent studies have shown that post-learning neuronal reactivation of dopaminergic neurons that are involved in memory acquisition is needed for LTM consolidation (18). Importantly, this reactivation necessitates sleep and the activity of vFB neurons during a narrow time window after learning (18, 53). Based on their data, the authors proposed that vFB and dFB neurons

promote sleep in response to different types of experiences and that these neurons underlie different functions of sleep (18). We wondered whether the sleep induced by activation of dFB$^{23E10\cap 84C10}$ neurons, which are involved in sleep homeostasis (Fig 3J and 3K), could convert STM to LTM. Thus, we used a 1h courtship training protocol that does not create LTM, and activated dFB$^{23E10\cap 84C10}$ neurons optogenetically for 23h following the end of training. LTM was tested 24h after the onset of training (Fig 5A). As seen in Fig 5B, sleep is significantly increased when activating dFB$^{23E10\cap 84C10}$ neurons post-training. When looking at LTM, control flies and *dFB-Split>CsChrimson* flies that were trained for 1h, but whose sleep was not increased following training, show no memory, as expected (Fig 5C). However, activating dFB$^{23E10\cap 84C10}$ neurons for 23h after a 1h courtship training session led to LTM, as indicated by a significantly higher Suppression Index (Fig 5C). Individual values of courtship indices for untrained and trained males are presented in S14A Fig. These data suggest that the sleep that is induced by activation of dFB$^{23E10\cap 84C10}$ neurons can convert STM to LTM. An alternative hypothesis is that activation of dFB$^{23E10\cap 84C10}$ neurons promotes LTM consolidation independently of sleep. To rule out this possibility, we sleep-deprived *dFB-Split>CsChrimson* flies following the 1h training session while they were optogenetically activated. This manipulation resulted in sleep loss (Fig 5B) and no LTM (Fig 5C). Thus, we conclude that the sleep that is induced by activation of dFB$^{23E10\cap 84C10}$ neurons can convert STM to LTM.

Discussion

The strength of the fly model lies in its strong genetic techniques, allowing researchers to selectively manipulate discrete populations of neurons and monitor how specific behaviors are affected. To do so, an impressive collection of binary expression systems have been developed.

In particular, the GAL4/UAS system (3) has been the keystone of *Drosophila* neurobiological studies. However, GAL4 drivers are often not specific enough and express in cells outside the region of interest. This can make the task of unequivocally assigning a given behavior to a specific neuron or group of neurons particularly difficult. Importantly, refinement of GAL4 expression can be achieved by employing the intersectional Split-GAL4 technology (6).

Like mammalian sleep, sleep in *Drosophila* is regulated by multiple areas in the brain (12, 13). An expanding amount of evidence supports a role for dFB neurons in sleep regulation (14-17, 20, 22, 24, 48, 54). The most widely used tool to manipulate dFB neurons is the 23E10-GAL4 driver (20, 21), and thermogenetic or optogenetic activation of 23E10-GAL4 neurons results in increased sleep (18, 24-27). However, we previously demonstrated that 23E10-GAL4 expresses in VNC-SP neurons, two cholinergic sleep-promoting neurons located in the VNC (27), putting the role of 23E10-GAL4 dFB neurons in question. The involvement of VNC-located neurons in 23E10-GAL4 sleep-promotion has been demonstrated further by a subsequent paper (28). Simply put, we think that 23E10-GAL4 should not be employed as a dFB-specific driver line anymore. The aforementioned study also went further by suggesting that the dFB plays no role at all in sleep (28), a conclusion we did not make based on the fact that we found that there are 23E10-GAL4 expressing neurons involved in sleep homeostasis that are different from VNC-SP neurons (27). However, whether these sleep homeostasis-regulating 23E10-GAL4 neurons are dFB neurons was uncertain. In this study, we sought to unequivocally assess the role of 23E10-GAL4 dFB neurons in sleep regulation.

To do so we adopted a targeted Split-GAL4 strategy combining 20 individual AD lines (selected for the strong dFB expression pattern of their GAL4 counterparts) with a 23E10-DBD line. We screened these 20 novel Split-GAL4 FBS lines behaviorally and anatomically. These experiments identified 7 FBS lines that strongly promote sleep when activated in females and males (Table S2). In addition, we found 9 lines that moderately modulate at least one sleep parameter (Table S2). Interestingly, only 4 FBS lines do not change any sleep parameter using both thermogenetic and optogenetic activation protocols (Table S2). An anatomical assessment of each line revealed that all sleep-promoting FBS lines express in dFB neurons (Table S1), as expected based on our targeted approach. However, they also express in the metathoracic ganglion of the VNC, especially in the previously described VNC-SP neurons (27). The high frequency of observation of these cells, and their very typical “bowtie” processes in the brain, in our FBS lines suggest that VNC-SP neurons are commonly expressed in many GAL4 lines. In fact, a MultiColor FlpOut (MCFO) study reported that neurons with similar projections (referred to as “sparse T” in this work) are observed in more than 60% of all Janelia GAL4 lines (55). The fact that these “bowtie” neurons are frequently present in many GAL4 lines probably explains why we see them in the vast majority of our FBS lines (17 out of 20 or 85% of them). This observation also highlights the need to use specific tools when trying to manipulate discrete neurons or groups of neurons. Since VNC-SP neurons are present in many GAL4 lines, it is likely that they are part of the expression pattern of GAL4 lines that have been used to manipulate diverse group of sleep-modulating neurons. Future studies using GAL4 lines in sleep studies will therefore need to take account of the potential presence of VNC-SP neurons in their expression pattern. Perhaps more importantly, existing data may need to be reinterpreted in light of our findings. Our study also found that the strength of expression within VNC-SP neurons

dictates how potent a given FBS line is in promoting sleep. However, the ubiquitous presence of VNC-SP cells in sleep-promoting FBS lines prevented us from unequivocally assessing the role of dFB neurons in sleep regulation using these lines.

Fortunately, we identified a dFB-specific Split-GAL4 line (dFB-Split), which expresses in most 23E10-GAL4 dFB neurons (dFB$^{23E10\cap 84C10}$ neurons). Using our standard optogenetic protocol, activation of dFB$^{23E10\cap 84C10}$ neurons does not modulate sleep. However, when we increased the intensity of optogenetic activation, we found that activating dFB$^{23E10\cap 84C10}$ neurons increases sleep in both males and females. Importantly, we demonstrated this sleep-induction effect using the single beam DAM2 system, the multibeam DAM5H monitor, and by video analysis, ruling out that we have mislabeled periods of micromovements, grooming, or feeding as sleep. In addition, we showed that activation of dFB$^{23E10\cap 84C10}$ neurons increase arousal threshold, indicating that flies sleep deeper when dFB$^{23E10\cap 84C10}$ neurons are activated. Importantly, though the sleep obtained by dFB$^{23E10\cap 84C10}$ neurons activation is deeper, it is reversible, an important hallmark of sleep.

Chronic hyperpolarization of dFB$^{23E10\cap 84C10}$ neurons interferes with sleep homeostasis. We found that expressing Kir2.1 in dFB$^{23E10\cap 84C10}$ neurons leads to a reduction in the amount of sleep that flies recover following sleep deprivation, when compared with controls. However, *dFB-Split>Kir2.1* flies show a modest, but significant sleep rebound, especially during the first hours in the recovery period. Interestingly, a recent study found that hyperpolarizing all 23E10-GAL4 neurons does not impair early (6h) sleep homeostasis (28). These data demonstrate that

dFB$^{23E10\cap 84C10}$ neurons are involved in sleep homeostasis but indicate that there are other sleep homeostasis-regulating neurons in the fly nervous system, a suggestion also made by others (56). Surprisingly, chronic silencing of dFB$^{23E10\cap 84C10}$ neurons increases sleep, confirming that dFB neurons modulate sleep. This effect is not caused by gross morphological defects created by the expression of Kir2.1 throughout the development and life of the flies. How do we explain this result? Previous studies have demonstrated that the level of connectivity between dFB neurons is high (49, 57). In addition, dFB$^{23E10\cap 84C10}$ neurons are neurochemically heterogeneous (see below), expressing glutamate and acetylcholine. Acetylcholine is the main excitatory neurotransmitter in the fly nervous system, but glutamate acts as an inhibitory neurotransmitter in dFB neurons (49) .We hypothesize that chronic hyperpolarization of all dFB$^{23E10\cap 84C10}$ neurons may lead to complex effects on the activity of individual cells in this heterogeneous population, leading to unexpected and complicated sleep phenotypes.

Why do dFB$^{23E10\cap 84C10}$ neurons require such a strong activation protocol to increase sleep? Considering that dFB neurons are subject to dopaminergic regulation (15, 17, 20, 44), we hypothesize that under baseline conditions, dFB neurons are under severe dopaminergic inhibition and that our standard optogenetic activation protocol is not sufficient to bring these cells above firing threshold. Increasing the intensity of the activation protocol reliably leads to sleep increases in what appears to be a direct relationship. Importantly, following 12h of sleep-deprivation, individual dFB neurons increase their firing frequencies, with some neurons capable of firing up to 50Hz (16). These data indicate that our optogenetic protocols, using 20Hz and 50Hz frequencies to activate dFB neurons, are within the physiological range of normal firing properties for these cells.

A recent preprint showed that optogenetic activation of dFB neurons, as labelled with a VGlut-AD; 23E10-DBD line, increased sleep when using an activation protocol consisting of 10 bursts of LED ON compressed in one half of a 500:500 ms duty cycle. Interestingly, a 10Hz activation, delivering the same number of light pulses spread evenly across time failed to increase sleep (49). The authors thus concluded that the temporal structure of the activation protocol used to activate dFB neurons is important to their sleep-promoting capacities (49). While we expect that the expression pattern of our dFB-Split driver and the VGlut-AD; 23E10-DBD line contains mostly similar neurons (since they both rely on 23E10-DBD), we suspect that they are not fully identical. These slight differences in expression pattern may explain the difference between our results and others (49), and further suggest that dFB neurons are heterogeneous (16). Illustrating this heterogeneity, we found that most dFB$^{23E10\cap 84C10}$ neurons express both glutamate and acetylcholine, while a minority of them only express one of these two neurotransmitters. Our behavioral data supports a major role in sleep-promotion for the cholinergic dFB$^{ChAT\cap 84C10}$ neurons. Activating glutamatergic dFB$^{VGlut\cap 84C10}$ neurons has a much milder effect on sleep, only increasing sleep during the day. We note that activation of VGlut-AD; 23E10-DBD expressing neurons also led to a modest sleep increase during the day (49). Interestingly, our study could not confirm previous work suggesting that dFB neurons are GABAergic (47, 48), using both a Split-GAL4 and immunocytochemistry approaches. Taken together, these data indicate that additional genetic dissection of individual dFB neurons will be needed to fully understand the contribution of neurochemically different dFB neurons to sleep regulation.

Finally, a previous study demonstrated that vFB neurons regulate learning-dependent sleep and that these cells play an essential role in LTM consolidation (18). The same work proposed that vFB and dFB neurons promote different types of sleep that may underlie different functions (18). While vFB and dFB neurons may promote sleep in response to different drives, a learning-dependent sleep drive for vFB neurons and a homeostatic sleep drive for dFB cells, we found that the sleep obtained by activation of dFB$^{23E10\cap 84C10}$ neurons can consolidate LTM. Thus, we conclude that the benefit of sleep on memory consolidation is not circuit-specific.

In conclusion, our work demonstrates that dFB are neurochemically heterogeneous and that these neurons modulate sleep, especially sleep homeostasis. In addition, dFB-generated sleep can consolidate LTM. Further work is needed to dissect the heterogeneous dFB population and will identify the contribution of individual dFB neurons in sleep regulation.

Materials and Methods

Drosophila stocks and rearing

Flies were cultured at 25˚C with 50% humidity under a 12h light:12h dark cycle. Flies were kept on a standard yeast and molasses diet (per 1L: 50g yeast, 15g sucrose, 28g corn syrup, 33.3mL molasses, 9g agar). Fly stocks used in this study are listed in Table S3.

Sleep behavioral experiments

Sleep was assessed as previously described (11, 19, 27). 4-10 day old virgin females or males were used as described in figure legends. Briefly, flies were placed into individual 65 mm tubes and all activity was continuously measured through the Trikinetics Drosophila Activity Monitoring System (DAM2, www.Trikinetics.com, Waltham, Ma). Locomotor activity was measured in 1-minute bins and sleep was defined as periods of quiescence lasting at least 5 minutes. For multibeam monitoring, we used the DAM5H monitors (www.Trikinetics.com, Waltham, Ma).

Quantitative Video analysis

Video recording was performed as previously described (27). Flies fed food supplemented with 400µM all-trans retinal (Sigma, #R2500) or vehicle were loaded into individual 65mm tubes and placed on custom-built platforms. One webcam for 2 platforms was used to record the flies for 30 minutes starting at ZT1 (one hour after lights turn on in the morning). Fly behavior was manually scored and categorized as walking, grooming, feeding, resting (inactivity < 5min), or sleeping (inactivity > 5min). Videos were recorded on consecutive days for baseline (LED OFF) and activation (LED ON). Three separate experiments were performed and the pooled data is shown.

Optogenetic activation

For optogenetic activation, flies expressing CsChrimson were loaded into individual 65mm tubes with food supplemented with 400µM all-trans retinal (Sigma, #R2500) or vehicle control and kept under 12h low-light/12h darkness conditions for 48h. Sleep was then monitored for 24h of

baseline measurements. To activate CSChrimson, flies were put under 627nm LEDs (LuxeonStar LXM2-PD01-0040) and set to different activation protocols. The standard intensity protocol is set to a pulse cycle of (5ms on, 95ms off) x 20 with a 4 second delay between pulse cycles. The light intensity of this protocol is 0.078mW/mm^2. For the 20Hz protocol a cycle of 5ms on, 45ms off flashing continuously was used (light intensity=0.118mW/mm^2). For 50Hz, a cycle of 5ms on, 15ms off flashing continuously was used (light intensity=0.252mW/mm^2). The light intensity of the LED constantly ON protocol is 0.565mW/mm^2. A photodiode sensor (S120C, Thorlabs) paired with a digital console (PM100D, Thorlabs) was used to measure light intensity.

Sleep deprivation assay

Sleep deprivation was performed as previously described (19, 27, 58, 59). Briefly, flies were placed into individual 65 mm tubes and the sleep-nullifying apparatus (SNAP) was used to sleep deprive flies for 12 hours during the dark phase. Sleep homeostasis was calculated for each individual fly as the ratio of the minutes of sleep gained above baseline during 48h of recovery sleep divided by the total min of sleep lost during 12 h of sleep deprivation.

Arousal threshold

Arousal threshold was measured on flies that were ontogenetically activated. Control flies and flies expressing CsChrimson were loaded into individual 65mm glass tubes containing food supplemented with 400 μM all-trans retinal (Sigma, #R2500) or vehicle control. After 3 days the tubes were placed onto custom 3D printed trays, 16 tubes per tray. Video of two trays was recorded using a Raspberry Pi NoIR camera. Arousal stimulus was provided by three coreless vibration motors (7x25mm) capable of 8,000-16,000rmp vibration. Vibration pattern and

intensity were controlled by a DRV2605 haptic controller (Adafruit) paired with a Raspberry Pi 3 Model B+. A custom program was written in python to control the video and motor vibration (code available upon request). The programmed sequence starts with turning video recording on. Ten minutes after recording starts the stimulus pattern begins. The DRV2605 vibration effect used is transition click (effects 62 to 58) starting at 20% intensity and increasing in 20% increments to 100% intensity. Vibration occurred for 200ms followed by 800ms no vibration repeating four times followed by a 15sec break before the next increasing stimulus starts. Video recording continued for 10 minutes after final vibration stimulus. This program repeated once per hour from ZT3 to ZT9. Videos were manually scored. Flies inactive during the 5 minutes directly before the stimulus began were scored as sleeping. Sleeping flies were then assessed for movement during the increasing intensity stimulus. Arousal was reported based on the percentage of flies moving at each vibration intensity. Arousal threshold was scored on consecutive days for baseline (LED OFF) and activation (LED ON).

Immunocytochemistry

Flies were cold anesthetized, brains and VNC were dissected in ice cold Schneider's Drosophila Medium (Gibco, 21720024), and blocked in 5% normal goat serum. Following blocking, flies were incubated overnight at 4˚C in primary antibody, washed in PBST, and incubated overnight at 4˚C in secondary antibody. Primary antibodies used were chicken anti-GFP (1:1000; Aves Labs, Inc, #GFP-1020), mouse anti-bruchpilot (1:50; Developmental Studies Hybridoma Bank (DSHB), nc82-s), mouse anti-ChAT (1:100; DSHB, Chat4b1-c), rabbit anti-vGlut (1:500; DiAntonio lab (60), Washington University), and rabbit anti-GABA (1:1000; Sigma-Aldrich, #A2052). Secondary antibodies used were goat anti-chicken AlexaFluor 488 (1:800; Invitrogen,

#A32931), goat anti-mouse AlexaFluor 555 (1:400; Invitrogen #A32727), goat anti-rabbit AlexaFluor 555 (1:400; Invitrogen, #A32732), goat anti-mouse AlexaFluor 633 (1:400; Invitrogen, $A21052), and goat anti-rabbit AlexaFluor 633 (1:400; Invitrogen, #A21071). Brains and VNCs were mounted on polylysine-treated slides in Vectashield H-1000 mounting medium. Imaging was performed on a Zeiss 510 meta confocal microscope using a Plan-Apochromat 20x or Plan-Neofluar 40x objective. Z-series images were acquired with a 1 µm slice size using the same settings (laser power, gain, offset) to allow for comparison across genotypes. Images were processed and analyzed using ImageJ.

For non-CNS adult tissues (wings, legs, ovaries, and guts). Flies were collected, fixed, and stained similarly as brains and VNCs but following incubation with secondary antibodies and washing 3 times with PBST, tissue was incubated with 10µM 4',6-Diamidino-2-Phenylindole, Dihydrochloride (DAPI) (Invitrogen D1306) for 15 minutes at room temperature. Tissues were then washed in PBST and mounted in Vectashield.

GFP-DD

For destabilized GFP (GFP-DD) experiments, flies expressing GFP-DD were maintained on standard food. Flies were transferred to food containing 1mM Trimethoprim (TMP) solution (T1225, Teknova) or DMSO as control. Following 24 hours on TMP or DMSO containing food, flies were cold anesthetized and brains and VNCs were dissected. Brains and VNCs were fixed in 4% paraformaldehyde, washed in PBST, and mounted on slides. Brains and VNCs were imaged on a Zeiss 510 meta confocal microscope using a Plan-Neofluar 40X objective. GFP intensity was measured in ImageJ.

Courtship Conditioning Protocol

Naïve males were collected upon eclosion and isolated into glass sleep tubes. 48+ hours prior to training, males were transferred into new glass sleep tubes containing either vehicle or all-trans retinal dissolved in food and loaded into monitors. The 24h period prior to training served as the baseline sleep measurement. Naïve males were transferred into 13 mm x 100 mm glass culture tubes with food at the bottom, with respective vehicle or all-trans retinal additions, and paired for 1h with a mated trainer female (trained group) or alone (untrained group). Males were then transferred back into sleep tubes on the respective diet and sleep was monitored for the 23h post-training period. Flies subjected to LED activation were placed under 627 nm LED light at 20 Hz (5 ms ON and 45 ms OFF continuous cycles) for the post-training period. The sleep deprived group experienced LED activation and sleep deprivation over the 23h post-training period using the SNAP (19, 27, 58, 59). 24h after the onset of training, male flies were placed into courtship chambers with a mated tester female and video recorded for the 10 minute testing period. The courtship index (CI) was calculated using CI = (Time Spent on Courtship Behaviors / Total Time of Test) * 100. The suppression index (SI) was then calculated using SI = 100 * (1 – (CI Trained / CI Untrained)). Trainer and tester female mating status was visually confirmed after *don juan*-GFP pairing prior to training.

Courtship Video Processing and Scoring

Courtship videos were recorded for 10 minutes at 20 fps through OBS Studio software. Videos were analyzed using FlyTracker software (61, 62) and outputs were saved as JAABA files. The visualization tool within FlyTracker was used to confirm the assignment of male and female flies

and any switches in labeling were corrected using this feature. The videos and corresponding output files were scored using JAABA, a MATLAB-based machine learning program (63). Positive and negative frame examples were used to train three different scoring classifiers: OriChase (includes orientation and chase), SingWing (singing and wing extension), and MountCop (includes mounting and copulation). The accuracy of these classifiers was verified by built-in ground truth data and comparison to hand-scored tests. JAABAPlot was used to output the CI for each male fly and the resulting SI was calculated from these values.

Statistical analysis

Statistical analyses were performed with Prism10 software (GraphPad). Normal distribution was assessed with the D'Agostino-Pearson test. Normally distributed data were analyzed with parametric statistics: t-test, one-way analysis of variance or two-way ANOVA followed by the planned pairwise multiple comparisons as described in the legends. For data that significantly differed from the normal distribution, non-parametric statistics were applied, including Mann-Whitney U test, Kruskal–Wallis test followed by Dunn's multiple test, and Wilcoxon signed-rank test. Some non-normally distributed data were subjected to log transformation or Box-Cox transformation before two-way ANOVA followed by planned pairwise multiple comparisons as described in the legends. When box plots are used, the bottom and top of each box represents the first and third quartile, and the horizontal line dividing the box is the median. The whiskers represent the 10th and 90th percentiles. All statistically different groups are defined as $*P < 0.05$, $**P<0.01$, $***P<0.001$ and $****P<0.0001$.

Acknowledgments: We thank Aaron DiAntonio, Kausik Si, Gerry Rubin, and Paul Shaw for sharing reagents and protocols.

Reference and Notes:

1. Park HG, Carmel JB. Selective Manipulation of Neural Circuits. Neurotherapeutics. 2016;13(2):311-24.
2. Moulin TC, Covill LE, Itskov PM, Williams MJ, Schioth HB. Rodent and fly models in behavioral neuroscience: An evaluation of methodological advances, comparative research, and future perspectives. Neurosci Biobehav Rev. 2021;120:1-12.
3. Brand AH, Perrimon N. Targeted gene expression as a means of altering cell fates and generating dominant phenotypes. Development. 1993;118(2):401-15.
4. Lai SL, Lee T. Genetic mosaic with dual binary transcriptional systems in Drosophila. Nat Neurosci. 2006;9(5):703-9.
5. Potter CJ, Tasic B, Russler EV, Liang L, Luo L. The Q system: a repressible binary system for transgene expression, lineage tracing, and mosaic analysis. Cell. 2010;141(3):536-48.
6. Luan H, Peabody NC, Vinson CR, White BH. Refined spatial manipulation of neuronal function by combinatorial restriction of transgene expression. Neuron. 2006;52(3):425-36.
7. Keene AC, Duboue ER. The origins and evolution of sleep. J Exp Biol. 2018;221(Pt 11).
8. Miyazaki S, Liu CY, Hayashi Y. Sleep in vertebrate and invertebrate animals, and insights into the function and evolution of sleep. Neurosci Res. 2017;118:3-12.
9. Borbely AA. A two process model of sleep regulation. Hum Neurobiol. 1982;1(3):195-204.
10. Hendricks JC, Finn SM, Panckeri KA, Chavkin J, Williams JA, Sehgal A, et al. Rest in Drosophila is a sleep-like state. Neuron. 2000;25(1):129-38.
11. Shaw PJ, Cirelli C, Greenspan RJ, Tononi G. Correlates of sleep and waking in Drosophila melanogaster. Science. 2000;287(5459):1834-7.
12. Shafer OT, Keene AC. The Regulation of Drosophila Sleep. Curr Biol. 2021;31(1):R38-R49.
13. Dissel S. Drosophila as a Model to Study the Relationship Between Sleep, Plasticity, and Memory. Front Physiol. 2020;11:533.
14. Donlea JM, Thimgan MS, Suzuki Y, Gottschalk L, Shaw PJ. Inducing sleep by remote control facilitates memory consolidation in Drosophila. Science. 2011;332(6037):1571-6.
15. Ueno T, Tomita J, Tanimoto H, Endo K, Ito K, Kume S, et al. Identification of a dopamine pathway that regulates sleep and arousal in Drosophila. Nat Neurosci. 2012;15(11):1516-23.
16. Donlea JM, Pimentel D, Miesenbock G. Neuronal Machinery of Sleep Homeostasis in Drosophila. Neuron. 2014;81(6):1442.
17. Liu Q, Liu S, Kodama L, Driscoll MR, Wu MN. Two dopaminergic neurons signal to the dorsal fan-shaped body to promote wakefulness in Drosophila. Curr Biol. 2012;22(22):2114-23.
18. Dag U, Lei Z, Le JQ, Wong A, Bushey D, Keleman K. Neuronal reactivation during post-learning sleep consolidates long-term memory in Drosophila. Elife. 2019;8.
19. Dissel S, Angadi V, Kirszenblat L, Suzuki Y, Donlea J, Klose M, et al. Sleep restores behavioral plasticity to Drosophila mutants. Curr Biol. 2015;25(10):1270-81.
20. Pimentel D, Donlea JM, Talbot CB, Song SM, Thurston AJF, Miesenbock G. Operation of a homeostatic sleep switch. Nature. 2016;536(7616):333-7.

811 21. Jenett A, Rubin GM, Ngo TT, Shepherd D, Murphy C, Dionne H, et al. A GAL4-driver line resource
812 for Drosophila neurobiology. Cell Rep. 2012;2(4):991-1001.
813 22. Kempf A, Song SM, Talbot CB, Miesenbock G. A potassium channel beta-subunit couples
814 mitochondrial electron transport to sleep. Nature. 2019;568(7751):230-4.
815 23. Alam MA, Kumar S, McGinty D, Alam MN, Szymusiak R. Neuronal activity in the preoptic
816 hypothalamus during sleep deprivation and recovery sleep. J Neurophysiol. 2014;111(2):287-99.
817 24. Qian Y, Cao Y, Deng B, Yang G, Li J, Xu R, et al. Sleep homeostasis regulated by 5HT2b receptor in
818 a small subset of neurons in the dorsal fan-shaped body of drosophila. Elife. 2017;6.
819 25. Yap MHW, Grabowska MJ, Rohrscheib C, Jeans R, Troup M, Paulk AC, et al. Oscillatory brain
820 activity in spontaneous and induced sleep stages in flies. Nat Commun. 2017;8(1):1815.
821 26. Berry JA, Cervantes-Sandoval I, Chakraborty M, Davis RL. Sleep Facilitates Memory by Blocking
822 Dopamine Neuron-Mediated Forgetting. Cell. 2015;161(7):1656-67.
823 27. Jones JD, Holder BL, Eiken KR, Vogt A, Velarde AI, Elder AJ, et al. Regulation of sleep by
824 cholinergic neurons located outside the central brain in Drosophila. PLoS Biol. 2023;21(3):e3002012.
825 28. De J, Wu M, Lambatan V, Hua Y, Joiner WJ. Re-examining the role of the dorsal fan-shaped body
826 in promoting sleep in Drosophila. Curr Biol. 2023;33(17):3660-8 e4.
827 29. Tirian L, Dickson BJ. The VT GAL4, LexA, and split-GAL4 driver line collections for targeted
828 expression in the *Drosophila* nervous system. BioRxiv 198648 [Preprint] October 5, 2017 Available from:
829 https://doiorg/101101/198648. 2017.
830 30. Dionne H, Hibbard KL, Cavallaro A, Kao JC, Rubin GM. Genetic Reagents for Making Split-GAL4
831 Lines in Drosophila. Genetics. 2018;209(1):31-5.
832 31. Hamada FN, Rosenzweig M, Kang K, Pulver SR, Ghezzi A, Jegla TJ, et al. An internal thermal
833 sensor controlling temperature preference in Drosophila. Nature. 2008;454(7201):217-20.
834 32. Klapoetke NC, Murata Y, Kim SS, Pulver SR, Birdsey-Benson A, Cho YK, et al. Independent optical
835 excitation of distinct neural populations. Nat Methods. 2014;11(3):338-46.
836 33. van Alphen B, Yap MH, Kirszenblat L, Kottler B, van Swinderen B. A dynamic deep sleep stage in
837 Drosophila. J Neurosci. 2013;33(16):6917-27.
838 34. Ishimoto H, Lark A, Kitamoto T. Factors that Differentially Affect Daytime and Nighttime Sleep in
839 Drosophila melanogaster. Front Neurol. 2012;3:24.
840 35. Lamaze A, Ozturk-Colak A, Fischer R, Peschel N, Koh K, Jepson JE. Regulation of sleep plasticity
841 by a thermo-sensitive circuit in Drosophila. Sci Rep. 2017;7:40304.
842 36. Parisky KM, Agosto Rivera JL, Donelson NC, Kotecha S, Griffith LC. Reorganization of Sleep by
843 Temperature in Drosophila Requires Light, the Homeostat, and the Circadian Clock. Curr Biol.
844 2016;26(7):882-92.
845 37. Kim JH, Ki Y, Lee H, Hur MS, Baik B, Hur JH, et al. The voltage-gated potassium channel Shaker
846 promotes sleep via thermosensitive GABA transmission. Commun Biol. 2020;3(1):174.
847 38. Isaac RE, Li C, Leedale AE, Shirras AD. Drosophila male sex peptide inhibits siesta sleep and
848 promotes locomotor activity in the post-mated female. Proc Biol Sci. 2010;277(1678):65-70.
849 39. Khericha M, Kolenchery JB, Tauber E. Neural and non-neural contributions to sexual dimorphism
850 of mid-day sleep in Drosophila melanogaster: a pilot study. Physiol Entomol. 2016;41(4):327-34.
851 40. Wu B, Ma L, Zhang E, Du J, Liu S, Price J, et al. Sexual dimorphism of sleep regulated by juvenile
852 hormone signaling in Drosophila. PLoS Genet. 2018;14(4):e1007318.
853 41. Kim H, Kirkhart C, Scott K. Long-range projection neurons in the taste circuit of Drosophila. Elife.
854 2017;6.
855 42. Dolan MJ, Luan H, Shropshire WC, Sutcliffe B, Cocanougher B, Scott RL, et al. Facilitating Neuron-
856 Specific Genetic Manipulations in Drosophila melanogaster Using a Split GAL4 Repressor. Genetics.
857 2017;206(2):775-84.

858 43. Sethi S, Wang JW. A versatile genetic tool for post-translational control of gene expression in
859 Drosophila melanogaster. Elife. 2017;6.
860 44. Dissel S, Klose MK, van Swinderen B, Cao L, Ford M, Periandri EM, et al. Sleep-promoting
861 neurons remodel their response properties to calibrate sleep drive with environmental demands. PLoS
862 Biol. 2022;20(9):e3001797.
863 45. Baines RA, Uhler JP, Thompson A, Sweeney ST, Bate M. Altered electrical properties in
864 Drosophila neurons developing without synaptic transmission. J Neurosci. 2001;21(5):1523-31.
865 46. Kitamoto T. Conditional modification of behavior in Drosophila by targeted expression of a
866 temperature-sensitive shibire allele in defined neurons. J Neurobiol. 2001;47(2):81-92.
867 47. Ni JD, Gurav AS, Liu W, Ogunmowo TH, Hackbart H, Elsheikh A, et al. Differential regulation of
868 the Drosophila sleep homeostat by circadian and arousal inputs. Elife. 2019;8.
869 48. Donlea JM, Pimentel D, Talbot CB, Kempf A, Omoto JJ, Hartenstein V, et al. Recurrent Circuitry
870 for Balancing Sleep Need and Sleep. Neuron. 2018;97(2):378-89 e4.
871 49. Hasenhuetl PS, Sarnataro R, Vrontou E, Rorsman HO, Talbot CB, Brain R, et al. A half-centre
872 oscillator encodes sleep pressure. bioRxiv. 2024:2024.02.23.581780.
873 50. Goel N, Rao H, Durmer JS, Dinges DF. Neurocognitive consequences of sleep deprivation. Semin
874 Neurol. 2009;29(4):320-39.
875 51. Diekelmann S, Born J. The memory function of sleep. Nat Rev Neurosci. 2010;11(2):114-26.
876 52. Denis D, Cairney SA. Neural reactivation during human sleep. Emerg Top Life Sci. 2023;7(5):487-
877 98.
878 53. Lei Z, Henderson K, Keleman K. A neural circuit linking learning and sleep in Drosophila long-
879 term memory. Nat Commun. 2022;13(1):609.
880 54. Tainton-Heap LAL, Kirszenblat LC, Notaras ET, Grabowska MJ, Jeans R, Feng K, et al. A
881 Paradoxical Kind of Sleep in Drosophila melanogaster. Curr Biol. 2021;31(3):578-90 e6.
882 55. Meissner GW, Nern A, Dorman Z, DePasquale GM, Forster K, Gibney T, et al. A searchable image
883 resource of Drosophila GAL4 driver expression patterns with single neuron resolution. Elife. 2023;12.
884 56. Satterfield LK, De J, Wu M, Qiu T, Joiner WJ. Inputs to the sleep homeostat originate outside the
885 brain. J Neurosci. 2022.
886 57. Hulse BK, Haberkern H, Franconville R, Turner-Evans DB, Takemura SY, Wolff T, et al. A
887 connectome of the Drosophila central complex reveals network motifs suitable for flexible navigation
888 and context-dependent action selection. Elife. 2021;10.
889 58. Seugnet L, Suzuki Y, Vine L, Gottschalk L, Shaw PJ. D1 receptor activation in the mushroom
890 bodies rescues sleep-loss-induced learning impairments in Drosophila. Curr Biol. 2008;18(15):1110-7.
891 59. Melnattur K, Morgan E, Duong V, Kalra A, Shaw PJ. The Sleep Nullifying Apparatus: A Highly
892 Efficient Method of Sleep Depriving Drosophila. J Vis Exp. 2020(166).
893 60. Daniels RW, Collins CA, Chen K, Gelfand MV, Featherstone DE, DiAntonio A. A single vesicular
894 glutamate transporter is sufficient to fill a synaptic vesicle. Neuron. 2006;49(1):11-6.
895 61. Barbaro BA, Lukacsovich T, Agrawal N, Burke J, Bornemann DJ, Purcell JM, et al. Comparative
896 study of naturally occurring huntingtin fragments in Drosophila points to exon 1 as the most pathogenic
897 species in Huntington's disease. Hum Mol Genet. 2015;24(4):913-25.
898 62. Barwell T, Raina S, Seroude L. Versatile method to measure locomotion in adult Drosophila.
899 Genome. 2021;64(2):139-45.
900 63. Kabra M, Robie AA, Rivera-Alba M, Branson S, Branson K. JAABA: interactive machine learning
901 for automatic annotation of animal behavior. Nat Methods. 2013;10(1):64-7.

902

Competing interests: The authors have no competing interests.

Data and materials availability: All data are available in the main text or the supplementary materials.

Figure Legends

Fig 1. Behavioral and anatomical screen of FBS lines.

A) Diagram of the experimental assay. Sleep was measured at 22°C (for thermogenetic activation) or with LED OFF (for the optogenetic activation protocol) for 2 days to establish baseline sleep profile. Flies were then shifted to 31°C (thermogenetic) or LEDs were turned ON (LED ON, optogenetic) for 24h at the start of day3 to increase activity of the targeted cells by activating the TrpA1 or CsChrimson channel, and then returned to 22°C or LED OFF on day4. White bars (L) represent the 12h of light and black bars (D) represent the 12h of dark that are oscillating daily.

B) Box plots of total sleep change in % ((total sleep on day3-total sleep on day2/total sleep on day2) X 100) for female control (Empty: Empty-AD; 23E10-DBD) and 20 FBS lines expressing UAS-TrpA1; UAS-mCD8GFP. The bottom and top of each box represents the first and third quartile, and the horizontal line dividing the box is the median. The whiskers represent the 10th and 90th percentiles. The gray rectangle spanning the horizontal axis indicates the interquartile range of the control. Kruskal-Wallis ANOVA followed by Dunn's multiple comparisons revealed that 4 FBS lines increase sleep significantly more than control flies when thermogenetically activated. *P<0.05, **P<0.01, ***P<0.001, ****P<0.0001, n=30-45 flies per genotype.

C) Box plots of total sleep change in % ((total sleep on day3-total sleep on day2/total sleep on day2) X 100) for vehicle-fed and retinal-fed control (Empty) and 20 FBS female flies expressing CsChrimson upon 627nm LED stimulation. The bottom and top of each box represents the first and third quartile, and the horizontal line dividing the box is the median. The whiskers represent the 10th and 90th percentiles. Two-way ANOVA followed by Sidak's multiple comparisons revealed that 6 retinal-fed FBS lines increase sleep significantly when stimulated with 627nm

LEDs when compared with vehicle-fed flies. **P<0.01, ***P<0.001, ****P<0.0001, n=20-40 flies per genotype and condition.

D-H) Left, sleep profile in minutes of sleep per hour for day 2 (22°C, blue line) and day 3 (31°C, red line) for empty control (Empty-AD; 23E10-DBD, **D**), FBS42 (**E**), FBS45 (**F**), FBS53 (**G**) and FBS68 (**H**) female flies expressing TrpA1 and mCD8GFP. Right, Representative confocal stacks for each *FBS>UAS-TrpA1; UAS-mCD8GFP* line of a female brain (left panel), VNC (middle panel) as well as a magnified view of the location of VNC-SP "bowtie" processes. Green, anti-GFP; magenta, anti-nc82 (neuropile marker).

The raw data underlying parts B and C can be found in S1 Data.

Fig 2. Activation of dFB$^{23E10\cap 84C10}$ neurons promotes sleep.

A) Representative confocal stack of a female *84C10AD; 23E10-DBD (dFB-Split)>UAS-mCD8GFP* brain (left panel), VNC (middle panel), and the location where VNC-SP "bowtie" processes are seen in many FBS lines, but not in dFB-Split (right panel). We observed 22.52 ± 0.59 (n=23) dFB neurons in *dFB-Split>UAS-mCD8GFP* brains. Green, anti-GFP; magenta, anti-nc82 (neuropile marker).

B) Sleep profile in minutes of sleep per hour for day 2 (LED OFF, blue line) and day 3 (LED ON, red line) for retinal-fed empty control (Empty-AD; 23E10-DBD) and dFB-Split female flies expressing CsChrimson subjected to our standard optogenetic activation protocol (5ms LED ON, 95ms LED OFF, with a 4 second delay between pulses).

C) Box plots of total sleep change in % ((total sleep on day3-total sleep on day2/total sleep on day2) X 100) for female control (Empty-AD; 23E10-DBD) and dFB-Split flies expressing CsChrimson under standard optogenetic activation. Two-way ANOVA followed by Sidak's multiple comparisons revealed no differences between control and dFB-Split. n.s.= not significant. n=59-82 flies per genotype and condition.

D) Box plots of total sleep change in % for male control (Empty-AD; 23E10-DBD) and dFB-Split flies expressing CsChrimson under standard optogenetic activation. Two-way ANOVA

followed by Sidak's multiple comparisons revealed no differences between control and dFB-Split. n.s.= not significant. n=30-62 flies per genotype and condition.

E) Sleep profile in minutes of sleep per hour for day 2 (LED OFF, blue line) and day 3 (LED ON, red line) for retinal-fed empty control (Empty-AD; 23E10-DBD) and dFB-Split female flies expressing CsChrimson subjected to a 20Hz optogenetic activation protocol (cycles of 5ms LED ON, 45ms LED OFF).

F) Box plots of total sleep change in % for female control (Empty-AD; 23E10-DBD) and dFB-Split flies expressing CsChrimson under 20Hz optogenetic activation. Two-way ANOVA followed by Sidak's multiple comparisons revealed that sleep is significantly increased in *dFB-Split>CsChrimson* females. **P<0.01, n.s.= not significant. n=26-38 flies per genotype and condition.

G) Box plots of total sleep change in % for male control (Empty-AD; 23E10-DBD) and dFB-Split flies expressing CsChrimson under 20Hz optogenetic activation. Two-way ANOVA followed by Sidak's multiple comparisons revealed that sleep is significantly increased in *dFB-Split>CsChrimson* males. n.s.= not significant, *P<0.05. n=31-41 flies per genotype and condition.

H) Sleep profile in minutes of sleep per hour for day 2 (LED OFF, blue line) and day 3 (LED ON, red line) for retinal-fed empty control (Empty-AD; 23E10-DBD) and dFB-Split female flies expressing CsChrimson subjected to a 50Hz optogenetic activation protocol (cycles of 5ms LED ON, 45ms LED OFF).

I) Box plots of total sleep change in % for female control (Empty-AD; 23E10-DBD) and dFB-Split flies expressing CsChrimson under 50Hz optogenetic activation. Two-way ANOVA followed by Sidak's multiple comparisons revealed that sleep is significantly increased in *dFB-Split>CsChrimson* females. *P<0.05, ***P<0.001. n=25-38 flies per genotype and condition.

J) Box plots of total sleep change in % for male control (Empty-AD; 23E10-DBD) and dFB-Split flies expressing CsChrimson under 50Hz optogenetic activation. Two-way ANOVA followed by Sidak's multiple comparisons revealed that sleep is significantly increased in *dFB-Split>CsChrimson* males. n.s.= not significant, ***P<0.001. n=62-73 flies per genotype and condition.

K) Box plots of total sleep change in % for female control (Empty-AD; 23E10-DBD) and dFB-Split flies expressing CsChrimson under 50Hz optogenetic activation obtained with the DAM5H multibeam system. Two-way ANOVA followed by Sidak's multiple comparisons revealed that sleep is significantly increased in *dFB-Split>CsChrimson* females. *P<0.05, **P<0.01. n=35-54 flies per genotype and condition.

L) Box plots of total sleep change in % for female control (Empty-AD; 23E10-DBD) and dFB-Split flies expressing CsChrimson under constant optogenetic activation. Two-way ANOVA followed by Sidak's multiple comparisons revealed that sleep is significantly increased in *dFB-Split>CsChrimson* females. n.s.= not significant, ****P<0.0001. n=17-27 flies per genotype and condition.

M) Video analysis of retinal-fed control and *dFB-Split>UAS-CsChrimson* female flies. Recording was performed at ZT1-2 for 30 minutes on consecutive days during baseline (OFF) and activation (ON). Behaviors were manually scored, and amount of time spent in each behavior over 30 minutes is shown. Two-way ANOVA followed by Sidak's multiple comparisons test found that retinal-fed *dFB-Split>UAS-CsChrimson* flies with LED ON sleep significantly more than on baseline day (OFF), **** P<0.0001, but spend less time walking (**** P<0.0001), grooming (*** P<0.01), or feeding (**** P<0.0001). Rest (periods of inactivity shorter than 5 minutes) are not different. We observed no differences in time spent in all behaviors for control flies between activation and baseline days. n.s.= not significant. n= 8 flies for each genotype and condition.

N) Arousal threshold in vehicle-fed and retinal-fed *dFB-Split>UAS-CsChrimson* female flies. Percentage of flies awakened by a stimulus of increasing strength (20%, 40%, 60%, 80% or 100% of maximum strength) with and without 627nm LEDs stimulation. Two-way ANOVA followed by Sidak's multiple comparisons indicates that activation of $dFB^{23E10\cap 84C10}$ neurons reduce the responsiveness to the 20% and 40% stimulus strength when compared with non-activated flies. No difference in responsiveness is seen at the strongest stimulus (60%, 80% and 100%). Two-way ANOVA followed by Sidak's multiple comparisons indicates that in vehicle-fed flies no difference in responsiveness is seen between LED stimulated and non-stimulated

flies. ****P<0.0001, ***P<0.001, n.s.= not significant. n=16-33 flies per genotype and condition.

The raw data underlying parts C, D, F, G, I, J, K, L, M, and N can be found in S1 Data.

Fig 3. Chronic hyperpolarization of dFB$^{23E10\cap 84C10}$ neurons promotes sleep and impairs sleep homeostasis.

A) Sleep profile in minutes of sleep per hour for control (*Empty-AD; 23E10-DBD>UAS-Kir2.1*, blue line) and *dFB-Split>Kir2.1* (red line) female flies.

B) Box plots of total sleep (in minutes) for control and *dFB-Split>Kir2.1* female flies. A Two-tailed unpaired t test revealed that *dFB-Split>Kir2.1* female flies sleep significantly more than controls. **P<0.01. n=49-57 flies per genotype.

C) Box plots of locomotor activity counts per minute awake for flies presented in B. A Two-tailed unpaired t test revealed no differences between controls and *dFB-Split>Kir2.1* female flies. n.s.= not significant. n=49-57 flies per genotype.

D) Box plots of daytime sleep bout duration (in minutes) for flies presented in B. A Two-tailed Mann-Whitney U test revealed that daytime sleep bout duration is increased in *dFB-Split>Kir2.1* female flies. **P<0.01. n=49-57 flies per genotype.

E) Box plots of nighttime sleep bout duration (in minutes) for flies presented in B. A Two-tailed Mann-Whitney U test revealed no differences between controls and *dFB-Split>Kir2.1* female flies. n.s.= not significant. n=49-57 flies per genotype.

F) Box plots of total sleep (in minutes) for control and *dFB-Split>Kir2.1* female flies measured with the DAM5H multibeam system. A Two-tailed Mann-Whitney U test revealed that *dFB-Split>Kir2.1* female flies sleep significantly more than controls. ***P<0.001. n=49-61 flies per genotype.

G) Diagram of the experimental assay for acute silencing. Sleep was measured at 22°C for 2 days to establish baseline sleep profile. Flies were then shifted to 31°C for 24h at the start of day3 to silence the activity of the targeted cells by activating the Shi^{ts1} actuator, and then

returned to 22°C on day4. White bars (L) represent the 12h of light and black bars (D) represent the 12h of dark that are oscillating daily.

H) Box plots of total sleep change in % for control (*Empty-AD; 23E10-DBD>UAS-Shi*^{ts1}), and *dFB-Split>UAS-Shi*^{ts1} female flies upon thermogenetic silencing. A Two-tailed unpaired t test revealed no differences between controls and *dFB-Split>UAS-Shi*^{ts1} female flies. n.s.= not significant. n=50 flies per genotype.

I) Box plots of total sleep change in % for control (*Empty-AD; 23E10-DBD>UAS-Shi*^{ts1}), and *dFB-Split>UAS-Shi*^{ts1} male flies upon thermogenetic silencing. A Two-tailed unpaired t test revealed no differences between controls and *dFB-Split>UAS-Shi*^{ts1} male flies. n.s.= not significant. n=60-62 flies per genotype.

J) Cumulative sleep lost then gained for *Empty-AD; 23E10-DBD>UAS-Kir2.1* and *dFB-Split>UAS-Kir2.1* female flies during 12h of mechanical sleep deprivation (D+SD) and 48h of sleep recovery.

K) Box plots of total sleep recovered in % during 48h of sleep recovery following 12h of sleep deprivation at night for *Empty-AD; 23E10-DBD>UAS-Kir2.1* and *dFB-Split>UAS-Kir2.1* female flies. Two-tailed Mann-Whitney U tests revealed that sleep rebound is significantly decreased at all time points between controls and *dFB-Split>UAS-Kir2.1* female flies. However, Wilcoxon signed-rank tests (indicated by $^{\#}$ on graph) using $H_{0:}$ % sleep recovered = 0 revealed that *dFB-Split>UAS-Kir2.1* female flies have a sleep rebound significantly greater than 0 at time points 4h, 6h, 12h, and 24h. ***P<0.001, ****P<0.0001, $^{\#\#\#\#}$P<0.0001, $^{\#\#\#}$P<0.001, $^{\#}$P<0.5, n.s.= not significant. n=25-54 flies per genotype.

The raw data underlying parts B, C, D, E, F, H, I, J, and K can be found in S1 Data.

Fig 4. Neurochemical identity of dFB$^{23E10\cap 84C10}$ neurons.

A) Representative confocal stack of a female *dFB-Split>UAS-mCD8GFP* brain stained with GFP and GABA antibodies and focusing on dFB$^{23E10\cap 84C10}$ cell bodies. Green, anti-GFP; magenta, anti-GABA.

B) Representative confocal stack of a female *dFB-Split>UAS-mCD8GFP* brain stained with GFP, VGlut and ChAT antibodies and focusing on dFB$^{23E10\cap 84C10}$ cell bodies. White arrows indicate VGlut only positive dFB$^{23E10\cap 84C10}$ neurons. Yellow arrow shows a ChAT only positive dFB$^{23E10\cap 84C10}$ neuron. White asterisks indicate dFB$^{23E10\cap 84C10}$ neurons positive for VGlut and ChAT. Green, anti-GFP; blue, anti-VGlut, magenta, anti-ChAT.

C) Quantification of VGlut only positive, ChAT only positive and VGlut and ChAT positive dFB$^{23E10\cap 84C10}$ neurons. We observed 22.76± 0.58 (n=13) GFP positive dFB$^{23E10\cap 84C10}$ neurons per brain, 3.31± 0.71 cells were ChAT only positive, 4.69± 0.73 cells were VGlut only positive, 13.77± 0.93 cells were ChAT and VGlut positive, and 0.85± 0.25 cells were negative for both ChAT and VGlut.

D) Representative confocal stack of a female *84C10-AD; Gad1-DBD>UAS-mCD8GFP*. Green, anti-GFP; magenta, anti-nc82 (neuropile marker).

E) Representative confocal stack of a female *84C10-AD; ChAT-DBD>UAS-mCD8GFP*. Green, anti-GFP; magenta, anti-nc82 (neuropile marker).

F) Representative confocal stack of a female *VGlut-AD; 84C10-DBD>UAS-mCD8GFP*. Green, anti-GFP; magenta, anti-nc82 (neuropile marker).

G) Quantification of the numbers of dFB neurons contained within the 3 Split-GAL4 lines presented in D, E, and F. We observed no expression at all in *84C10-AD; Gad1-DBD* brains and VNC. 16.00± 0.41 (n=4) dFB cells for *84C10-AD; ChAT-DBD* and 22.20± 0.49 (n=5) dFB neurons for *VGlut-AD; 84C10-DBD.* No other expression was seen in the brain and VNC for these lines.

H) Sleep profile in minutes of sleep per hour for day 2 (LED OFF, blue line) and day 3 (LED ON, red line) for retinal-fed Empty-Split control females expressing CsChrimson subjected to a 50Hz optogenetic activation protocol (cycles of 5ms LED ON, 45ms LED OFF).

I) Sleep profile in minutes of sleep per hour for day 2 (LED OFF, blue line) and day 3 (LED ON, red line) for retinal-fed *VGlut-AD; 84C10-DBD>CsChrimson* female flies subjected to a 50Hz optogenetic activation protocol (cycles of 5ms LED ON, 45ms LED OFF).

J) Sleep profile in minutes of sleep per hour for day 2 (LED OFF, blue line) and day 3 (LED ON, red line) for retinal-fed *84C10-AD; ChAT-DBD>CsChrimson* female flies subjected to a 50Hz optogenetic activation protocol (cycles of 5ms LED ON, 45ms LED OFF).

K) Box plots of total sleep change in % ((total sleep on activation day-total sleep on baseline day/total sleep on baseline day) X 100) for control (*Empty-Split>CsChrimson*), *VGlut-AD; 84C10-DBD>CsChrimson* and *84C10-AD; ChAT-DBD>CsChrimson* female flies under a 50Hz optogenetic activation protocol. Two-way ANOVA followed by Sidak's multiple comparisons revealed that activating 84C10-AD; ChAT-DBD neurons significantly increases sleep. n.s.= not significant, ****P<0.0001. n=32-47 flies per genotype and condition.

L) Box plots of daytime sleep change in % ((daytime sleep on activation day-daytime sleep on baseline day/daytime sleep on baseline day) X 100) for control (*Empty-Split>CsChrimson*), *VGlut-AD; 84C10-DBD>CsChrimson* and *84C10-AD; ChAT-DBD>CsChrimson* female flies under a 50Hz optogenetic activation protocol. Two-way ANOVA followed by Tukey's multiple comparisons revealed that activating 84C10-AD; ChAT-DBD and VGlut-AD; 84C10-DBD neurons significantly increases daytime sleep and that activating 84C10-AD; ChAT-DBD neurons increase sleep more than activation of VGlut-AD; 84C10-DBD cells. n.s.= not significant, ***P<0.001, ****P<0.0001. n=32-47 flies per genotype and condition.

M) Box plots of locomotor activity counts per minute awake for retinal-fed flies presented in H. Two-way repeated measures ANOVA followed by Sidak's multiple comparisons revealed that activating 84C10-AD; ChAT-DBD neurons significantly increases locomotion when the flies are awake. n.s.= not significant, **P<0.01, ****P<0.0001. n=33-47 flies per genotype.

N) Box plots of locomotor activity counts per minute awake for vehicle-fed flies presented in H. Two-way repeated measures ANOVA followed by Sidak's multiple comparisons revealed no differences in waking activity. n.s.= not significant. n=32-45 flies per genotype.

The raw data underlying parts C, G, K, L, M, and N can be found in S1 Data.

Fig 5. The sleep induced by dFB$^{23E10\cap 84C10}$ neurons activation can consolidate Long-Term Memory.

A) Schematic of protocol for LTM consolidation. A 1 h training period that only generates STM is followed by optogenetic activation of dFB$^{23E10\cap 84C10}$ neurons for 23 h post-training (with or without sleep deprivation). Flies were tested 24 h after the onset of training.

B) Post-training sleep change for different genotypes and condition. The ~23 h time period post-training was matched to the equivalent time period on the baseline day for comparison. Unpaired parametric t-test for Empty-Split groups. Kruskal-Wallis test of multiple comparisons for dFB-Split groups using the vehicle condition as the control. ****P<0.0001, **P<0.01, ns= not significant. n= 46-54 flies per genotype and condition.

C) Courtship LTM shown as the suppression index (SI, SI = 100 * (1 – (CI Trained / CI Untrained))) of trained fly groups tested 24 h after the onset of training. Wilcoxon signed-rank test using $H_{0:}$ SI = 0. Sample size (untrained:trained) from left to right on the graph, n = 54 (27:27), 51 (27:24), 49 (27:22), 51 (26:25), 46 (21:25), and 53 (27:26), respectively. Courtship indices < 10% were excluded from both groups. ***P< 0.001, ns= not significant.

The raw data underlying parts B and C can be found in S1 Data.

Supporting Information

S1 Fig. Additional sleep profiles and confocal images of FBS lines.

A-P) Sleep profile (left) and representative confocal stacks (right) for brain and VNC of female *FBS>UAS-TrpA1; UAS-mCD8GFP* for 16 FBS lines not presented in Fig 1.

S2 Fig. Additional sleep parameters for FBS female flies thermogenetically activated.

A) Box plots of locomotor activity counts per minute awake for flies presented in Fig 1B. The bottom and top of each box represents the first and third quartile, and the horizontal line dividing the box is the median. The whiskers represent the 10th and 90th percentiles. Two-way repeated

measures ANOVA followed by Sidak's multiple comparisons test found that for 2 sleep-promoting FBS lines (FBS45 and FBS53) locomotor activity per awake time is increased while no differences are seen for the other 2 sleep-promoting lines between 22°C and 31°C. **P<0.01, ****P<0.0001, n=30-45 flies per genotype.

B) Box plots of daytime sleep bout duration in minutes for flies presented in Fig 1B. Two-way repeated measures ANOVA followed by Sidak's multiple comparisons test revealed that 7 FBS lines show a significant increase in daytime sleep bout duration between 22°C and 31°C. *P<0.05, **P<0.01, ***P<0.001, ****P<0.0001, n=30-45 flies per genotype.

C) Box plots of nighttime sleep bout duration in minutes for flies presented in Fig 1B. Two-way repeated measures ANOVA followed by Sidak's multiple comparisons test revealed that control and most FBS lines show a significant decrease in nighttime sleep bout duration between 22°C and 31°C. Only 4 sleep-promoting FBS lines show no difference between 22°C and 31°C. Dunnett's multiple comparisons reveal that for 3 of them, nighttime sleep bout duration at 31°C is significantly increased compared with Empty control flies (# on figure). **P<0.01, ***P<0.001, ****P<0.0001, n.s.= not significant. n=30-45 flies per genotype.

The raw data underlying parts A, B, and C can be found in S1 Data.

S3 Fig. Thermogenetic activation in male flies.

A) Box plots of total sleep change in % ((total sleep on day3-total sleep on day2/total sleep on day2) X 100) for male control (Empty-AD; 23E10-DBD) and 20 FBS lines expressing UAS-TrpA1; UAS-mCD8GFP. The gray rectangle spanning the horizontal axis indicates the interquartile range of the control. Kruskal-Wallis ANOVA followed by Dunn's multiple comparisons revealed that 7 FBS lines increase sleep significantly more than control flies when transferred to 31°C. *P<0.05, ****P<0.0001, n=26-47 flies per genotype.

B) Box plots of locomotor activity counts per minute awake for flies presented in A. Two-way repeated measures ANOVA followed by Sidak's multiple comparisons test found that for 3 sleep-promoting FBS lines (FBS45, FBS53 and FBS68) locomotor activity per awake time is increased while no differences are seen for the other 4 sleep-promoting lines between 22°C and 31°C. *P<0.05, **P<0.01, ***P<0.001, ****P<0.0001, n=26-47 flies per genotype.

C) Box plots of daytime sleep bout duration for flies presented in A. Two-way repeated measures ANOVA followed by Sidak's multiple comparisons test found that for 6 out of the 7 sleep-promoting FBS lines, daytime sleep bout duration is significantly increased at 31°C compared with 22°C. **P<0.01, ***P<0.001, ****P<0.0001, n=26-47 flies per genotype.

D) Box plots of nighttime sleep bout duration for flies presented in A. Two-way repeated measures ANOVA followed by Sidak's multiple comparisons revealed that control and most FBS lines show a significant decrease in nighttime sleep bout duration between 22°C and 31°C. 4 sleep-promoting FBS lines show no difference between 22°C and 31°C (FBS42, FBS53, FBS81 and FBS84) while FBS45 and FBS68 show an increase in nighttime sleep bout duration at 31°C. **P<0.01, ****P<0.0001, n=26-47 flies per genotype.

The raw data underlying parts A, B, C, and D can be found in S1 Data.

S4 Fig. Optogenetic activation in males.

A) Box plots of total sleep change in % ((total sleep on day3-total sleep on day2/total sleep on day2) X 100) for control (Empty) and 20 experimental vehicle-fed and retinal-fed male flies expressing CsChrimson upon 627nm LED stimulation. Two-way ANOVA followed by Sidak's multiple comparisons revealed that 8 retinal-fed FBS lines increase sleep significantly when stimulated with 627nm LEDs when compared with vehicle-fed flies. *P<0.05, **P<0.01, ****P<0.0001. n=20-44 flies per genotype and condition.

B) Box plots of locomotor activity counts per minute awake for retinal-fed flies presented in A. Two-way repeated measures ANOVA followed by Sidak's multiple comparisons test found that for most sleep-promoting FBS lines, locomotor activity per awake time is not affected when the flies are stimulated with 627nm LEDs while it is increased in *FBS72>UAS-CsChrimson* flies. *P<0.05, n=24-44 flies per genotype.

C) Box plots of daytime sleep bout duration (in minutes) for retinal-fed flies presented in A. Two-way repeated measures ANOVA followed by Sidak's multiple comparisons indicate that daytime sleep bout duration is increased in 11 FBS lines expressing CsChrimson when stimulated with 627nm LEDs. *P<0.05, ***P<0.001, ****P<0.0001, n=24-44 flies per genotype.

D) Box plots of nighttime sleep bout duration (in minutes) for retinal-fed flies presented in A. Two-way repeated measures ANOVA followed by Sidak's multiple comparisons indicate that nighttime sleep bout duration is increased in 6 FBS lines expressing CsChrimson when stimulated with 627nm LEDs. **P<0.01, ****P<0.0001, n=24-44 flies per genotype.

The raw data underlying parts A, B, C, and D can be found in S1 Data.

S5 Fig. Additional data for retinal-fed females in optogenetic activation.

A) Box plots of locomotor activity counts per minute awake for retinal-fed flies presented in Fig 1C. The bottom and top of each box represents the first and third quartile, and the horizontal line dividing the box is the median. The whiskers represent the 10th and 90th percentiles. Two-way repeated measures ANOVA followed by Sidak's multiple comparisons test found that for most sleep-promoting FBS lines, locomotor activity per awake time is not affected when the flies are stimulated with 627nm LEDs while it is increased in *FBS45>UAS-CsChrimson* flies. ****P<0.0001, n=21-40 flies per genotype.

B) Box plots of daytime sleep bout duration (in minutes) for retinal-fed flies presented in Fig 1C. The bottom and top of each box represents the first and third quartile, and the horizontal line dividing the box is the median. The whiskers represent the 10th and 90th percentiles. Two-way repeated measures ANOVA followed by Sidak's multiple comparisons indicate that daytime sleep bout duration is increased in 9 FBS lines expressing CsChrimson when stimulated with 627nm LEDs. *P<0.05, **P<0.01, ***P<0.001, ****P<0.0001, n=21-40 flies per genotype.

C) Box plots of nighttime sleep bout duration (in minutes) for retinal-fed flies presented in Fig 1C. The bottom and top of each box represents the first and third quartile, and the horizontal line dividing the box is the median. The whiskers represent the 10th and 90th percentiles. Two-way repeated measures ANOVA followed by Sidak's multiple comparisons indicate that nighttime sleep bout duration is increased in 6 FBS lines expressing CsChrimson when stimulated with 627nm LEDs. *P<0.05, ****P<0.0001, n=21-40 flies per genotype.

The raw data underlying parts A, B, and C can be found in S1 Data.

S6 Fig. Vehicle-fed sleep data for females in optogenetic experiments.

A) Box plots of locomotor activity counts per minute awake for vehicle-fed flies presented in Fig 1C. Two-way repeated measures ANOVA followed by Sidak's multiple comparisons test found that all lines except FBS42 show no difference in locomotor activity per awake time when the flies are stimulated with 627nm LEDs. ***P<0.001. n=20-39 flies per genotype.

B) Box plots of daytime sleep bout duration for vehicle-fed flies presented in Fig 1C. Two-way repeated measures ANOVA followed by Sidak's multiple comparisons test found that most vehicle-fed sleep-promoting lines show no difference in daytime sleep bout duration when the flies are stimulated with 627nm LEDs. *P<0.05, **P<0.01, ***P<0.001. n=20-39 flies per genotype.

C) Box plots of nighttime sleep bout duration for vehicle-fed flies presented in Fig 1C. Two-way repeated measures ANOVA followed by Sidak's multiple comparisons test show no difference in nighttime sleep bout duration when vehicle-fed flies are stimulated with 627nm LEDs. n=20-39 flies per genotype.

The raw data underlying parts A, B, and C can be found in S1 Data.

S7 Fig. Vehicle-fed sleep data for males in optogenetic experiments.

A) Box plots of locomotor activity counts per minute awake for vehicle-fed flies presented in Fig S4A. Two-way repeated measures ANOVA followed by Sidak's multiple comparisons test found no difference in locomotor activity per awake time when the flies are stimulated with 627nm LEDs. n=20-40 flies per genotype.

B) Box plots of daytime sleep bout duration for vehicle-fed flies presented in Fig S4A. Two-way repeated measures ANOVA followed by Sidak's multiple comparisons test found that most vehicle-fed sleep-promoting lines show no difference in daytime sleep bout duration when the flies are stimulated with 627nm LEDs. *P<0.05, **P<0.01, ****P<0.0001. n=20-40 flies per genotype.

C) Box plots of nighttime sleep bout duration for vehicle-fed flies presented in Fig S4A. Two-way repeated measures ANOVA followed by Sidak's multiple comparisons test show no

difference in nighttime sleep bout duration when vehicle-fed flies are stimulated with 627nm LEDs. n=20-40 flies per genotype.

The raw data underlying parts A, B, and C can be found in S1 Data.

S8 Fig. VNC-SP neurons are present in sleep-promoting FBS lines.

A) Representative confocal stacks of *FBS42>UAS-GFP* (left) and *FBS42>UAS-GFP; ChAT-LexA>2x LexAop2KZip*$^{+}$ (right) female flies showing the location of the VNC-SP bowtie processes, the dFB region, the VNC and VNC-SP neurons. Expression of GFP in VNC-SP neurons and in their bowtie brain processes is abolished by the expression of the KZip^{+} repressor. Gray arrows show VNC-SP neurons. Green, anti-GFP; magenta, anti-nc82.

B) Representative confocal stacks of *FBS45>UAS-GFP* (left) and *FBS45>UAS-GFP; ChAT-LexA> LexAop2KZip*$^{+}$ (right) female flies showing the location of the VNC-SP bowtie processes, the dFB region, the VNC and VNC-SP neurons. Expression of GFP in VNC-SP neurons and in their bowtie brain processes is abolished by the expression of the KZip^{+} repressor. Gray arrows show VNC-SP neurons. Green, anti-GFP; magenta, anti-nc82.

C) Representative confocal stacks of *FBS53>UAS-GFP* (left) and *FBS53>UAS-GFP; ChAT-LexA> LexAop2KZip*$^{+}$ (right) female flies showing the location of the VNC-SP bowtie processes, the dFB region, the VNC and VNC-SP neurons. Expression of GFP in VNC-SP neurons and in their bowtie brain processes is abolished by the expression of the KZip^{+} repressor. Gray arrows show VNC-SP neurons. Green, anti-GFP; magenta, anti-nc82.

D) Representative confocal stacks of *FBS68>UAS-GFP* (left) and *FBS68>UAS-GFP; ChAT-LexA> 2x LexAop2KZip*$^{+}$ (right) female flies showing the location of the VNC-SP bowtie processes, the dFB region, the VNC and VNC-SP neurons. Expression of GFP in VNC-SP neurons and in their bowtie brain processes is abolished by the expression of the KZip^{+} repressor. Gray arrows show VNC-SP neurons. Green, anti-GFP; magenta, anti-nc82.

E) Box plots of total sleep change in % ((total sleep on day3-total sleep on day2/total sleep on day2) X 100) for female control (Empty: Empty-AD; 23E10-DBD) and 4 sleep-promoting FBS lines expressing UAS-TrpA1 or UAS-TrpA1 and the KZip^{+} repressor in cholinergic neurons

(ChAT-KZip^{+}). Two-way ANOVA followed by Sidak's multiple comparisons revealed that repressing the expression of TrpA1 in cholinergic neurons abolishes the sleep increases obtained when thermogenetically activating all 4 FBS lines. ****P<0.0001, n.s.= not significant. $^{\#}$ indicates that sleep is significantly increased compared with *Empty>TrpA1* controls. n=17-69 flies per genotype.

The raw data underlying part E can be found in S1 Data.

S9 Fig. Differential strength of expression in VNC-SP neurons for different FBS lines.

A) Schematic of the GFP.DD experimental design.

B) Representative confocal stacks of females 23E10-GAL4, VNC-SP Split, FBS1, FBS33, FBS45, and FBS58 expressing GFP-DD and fed DMSO or TMP for 24h before dissection. Stacks are focused on the metathoracic region of the VNC where VNC-SP cell bodies are located. Green, anti-GFP.

C) Quantification of staining intensity for data presented in B. Two-way ANOVA followed by Sidak's multiple comparisons revealed that there is significantly more GFP staining in VNC-SP neurons in 23E10-GAL4, VNC-SP Split, FBS33, and FBS45 fed TMP compared with DMSO fed flies. **P<0.01, ****P<0.0001, n.s= not significant. n=5-14 VNC per genotype and condition.

The raw data underlying part C can be found in S1 Data.

S10 Fig. Expression pattern of dFB-Split.

Representative confocal stack images of adult tissues from *Empty-AD; 23E10-DBD > UAS-mCD8GFP* (top) and *dFB-Split> UAS-mCD8GFP* (bottom) female flies. GFP is expressed in the brain, but not the wings, legs, ovaries, or gut in dFB-Split. Tissue was dissected, fixed, and stained with DAPI. Green, anti-GFP; Blue, DAPI.

S11 Fig. Additional data for optogenetic activation of dFB$^{23E10\cap 84C10}$ neurons at 20Hz.

A) Box plots of locomotor activity counts per minute awake for retinal-fed flies presented in Fig 2F. Two-way repeated measures ANOVA followed by Sidak's multiple comparisons test found no difference in locomotor activity per awake time when the flies are stimulated with 627nm LEDs. n.s.= not significant. n=34-38 flies per genotype.

B) Box plots of daytime sleep bout duration for retinal-fed flies presented in Fig 2F. Two-way repeated measures ANOVA followed by Sidak's multiple comparisons test found that daytime sleep bout duration is significantly increased in *dFB-Split>CsChrimson* female flies that are stimulated with 627nm LEDs. ****P<0.0001, n.s.= not significant. n=34-38 flies per genotype.

C) Box plots of nighttime sleep bout duration for retinal-fed flies presented in Fig 2F. Two-way repeated measures ANOVA followed by Sidak's multiple comparisons test found that nighttime sleep bout duration is significantly increased in *dFB-Split>CsChrimson* female flies that are stimulated with 627nm LEDs. *P<0.05, n.s.= not significant. n=34-38 flies per genotype.

D) Box plots of locomotor activity counts per minute awake for vehicle-fed flies presented in Fig 2F. Two-way repeated measures ANOVA followed by Sidak's multiple comparisons test found no difference in locomotor activity per awake time when the flies are stimulated with 627nm LEDs. n.s.= not significant. n=26-32 flies per genotype.

E) Box plots of daytime sleep bout duration for vehicle-fed flies presented in Fig 2F. Two-way repeated measures ANOVA followed by Sidak's multiple comparisons test found no difference in daytime sleep bout duration when the flies are stimulated with 627nm LEDs. n.s.= not significant. n=26-32 flies per genotype.

F) Box plots of nighttime sleep bout duration for vehicle-fed flies presented in Fig 2F. Two-way repeated measures ANOVA followed by Sidak's multiple comparisons test. ****P<0.0001. n=26-32 flies per genotype.

G) Box plots of locomotor activity counts per minute awake for retinal-fed flies presented in Fig 2G. Two-way repeated measures ANOVA followed by Sidak's multiple comparisons test found no difference in locomotor activity per awake time when the flies are stimulated with 627nm LEDs. n.s.= not significant. n=35-41 flies per genotype.

H) Box plots of daytime sleep bout duration for retinal-fed flies presented in Fig 2G. Two-way repeated measures ANOVA followed by Sidak's multiple comparisons test found that daytime sleep bout duration is significantly increased in *dFB-Split>CsChrimson* male flies that are stimulated with 627nm LEDs. ****P<0.0001, n.s.= not significant. n=35-41 flies per genotype.

I) Box plots of nighttime sleep bout duration for retinal-fed flies presented in Fig 2G. Two-way repeated measures ANOVA followed by Sidak's multiple comparisons test found that nighttime sleep bout duration is significantly increased in *dFB-Split>CsChrimson* male flies that are stimulated with 627nm LEDs. ****P<0.0001, n.s.= not significant. n=35-41 flies per genotype.

J) Box plots of locomotor activity counts per minute awake for vehicle-fed flies presented in Fig 2G. Two-way repeated measures ANOVA followed by Sidak's multiple comparisons test. ***P<0.001, ****P<0.0001. n=31-36 flies per genotype.

K) Box plots of daytime sleep bout duration for vehicle-fed flies presented in Fig 2G. Two-way repeated measures ANOVA followed by Sidak's multiple comparisons test found no difference in vehicle-fed males. n.s.= not significant. n=31-36 flies per genotype.

L) Box plots of nighttime sleep bout duration for vehicle-fed flies presented in Fig 2G. Two-way repeated measures ANOVA followed by Sidak's multiple comparisons test show no difference in nighttime sleep bout duration when vehicle-fed flies are stimulated with 627nm LEDs. n.s.= not significant. n=31-36 flies per genotype.

The raw data underlying parts A, B, C, D, E, F, G, H, I, J, K, and L can be found in S1 Data.

S12 Fig. Additional data for optogenetic activation of dFB$^{23E10\cap 84C10}$ neurons at 50Hz.

A) Box plots of locomotor activity counts per minute awake for retinal-fed flies presented in Fig 2I. Two-way repeated measures ANOVA followed by Sidak's multiple comparisons test found no difference in locomotor activity per awake time in *dFB-Split>CsChrimson* female flies that are stimulated with 627nm LEDs. **P<0.01, n.s.= not significant. n=33-38 flies per genotype.

B) Box plots of daytime sleep bout duration for retinal-fed flies presented in Fig 2I. Two-way repeated measures ANOVA followed by Sidak's multiple comparisons test found that daytime

sleep bout duration is significantly increased in *dFB-Split>CsChrimson* female flies that are stimulated with 627nm LEDs. ****P<0.0001, n.s.= not significant. n=33-38 flies per genotype.

C) Box plots of nighttime sleep bout duration for retinal-fed flies presented in Fig 2I. Two-way repeated measures ANOVA followed by Sidak's multiple comparisons test found that nighttime sleep bout duration is significantly increased in *dFB-Split>CsChrimson* female flies that are stimulated with 627nm LEDs. ****P<0.0001, n.s.= not significant. n=33-38 flies per genotype.

D) Box plots of locomotor activity counts per minute awake for vehicle-fed flies presented in Fig 2I. Two-way repeated measures ANOVA followed by Sidak's multiple comparisons test. *P<0.05, n.s.= not significant. n=25-31 flies per genotype.

E) Box plots of daytime sleep bout duration for vehicle-fed flies presented in Fig 2I. Two-way repeated measures ANOVA followed by Sidak's multiple comparisons test found no difference in daytime sleep bout duration when the flies are stimulated with 627nm LEDs. n.s.= not significant. n=25-31 flies per genotype.

F) Box plots of nighttime sleep bout duration for vehicle-fed flies presented in Fig 2I. Two-way repeated measures ANOVA followed by Sidak's multiple comparisons test. **P<0.01, n.s.= not significant. n=25-31 flies per genotype.

G) Box plots of locomotor activity counts per minute awake for retinal-fed flies presented in Fig 2J. Two-way repeated measures ANOVA followed by Sidak's multiple comparisons test. ****P<0.0001, n.s.= not significant. n=62-71 flies per genotype.

H) Box plots of daytime sleep bout duration for retinal-fed flies presented in Fig 2J. Two-way repeated measures ANOVA followed by Sidak's multiple comparisons test found that daytime sleep bout duration is significantly increased in *dFB-Split>CsChrimson* female flies that are stimulated with 627nm LEDs. ****P<0.0001, n.s.= not significant. n=62-71 flies per genotype.

I) Box plots of nighttime sleep bout duration for retinal-fed flies presented in Fig 2J. Two-way repeated measures ANOVA followed by Sidak's multiple comparisons test show no difference in nighttime sleep bout duration when retinal-fed flies are stimulated with 627nm LEDs. n.s.= not significant. n=62-71 flies per genotype.

J) Box plots of locomotor activity counts per minute awake for vehicle-fed flies presented in Fig 2J. Two-way repeated measures ANOVA followed by Sidak's multiple comparisons test. **P<0.01, n.s.= not significant. n=63-73 flies per genotype.

K) Box plots of daytime sleep bout duration for vehicle-fed flies presented in Fig 2J. Two-way repeated measures ANOVA followed by Sidak's multiple comparisons test found no difference in daytime sleep bout duration when the flies are stimulated with 627nm LEDs. n.s.= not significant. n=63-73 flies per genotype.

L) Box plots of nighttime sleep bout duration for vehicle-fed flies presented in Fig 2J. Two-way repeated measures ANOVA followed by Sidak's multiple comparisons test. **P<0.01. n=63-73 flies per genotype.

The raw data underlying parts A, B, C, D, E, F, G, H, I, J, K, and L can be found in S1 Data.

S13 Fig. Additional data for hyperpolarization of dFB$^{23E10\cap 84C10}$ neurons.

A) Representative brain confocal stack of *dFB-Split>UAS-mCD8GFP*. Green, anti-GFP; magenta, anti-nc82.

B) Representative brain confocal stack of *dFB-Split>UAS-Kir2.1.EGFP*. We observed 23.40 ± 0.75 (n=5) dFB$^{23E10\cap 84C10}$ neurons in *dFB-Split>UAS-Kir2.1.EGFP* brains. This number is similar to what we have observed for *dFB-Split>UAS-mCD8GFP* brains (Fig 2A). Green, anti-GFP; magenta, anti-nc82.

C) Box plots of total sleep (in minutes) for control and *dFB-Split>Kir2.1* male flies. A Two-tailed Mann-Whitney U test revealed that *dFB-Split>Kir2.1* male flies sleep significantly more than controls. ****P<0.0001. n=69-75 flies per genotype.

D) Box plots of locomotor activity counts per minute awake for flies presented in C. A Two-tailed Mann-Whitney U test revealed no differences between controls and *dFB-Split>Kir2.1* male flies. n.s.= not significant. n=69-75 flies per genotype.

E) Box plots of daytime sleep bout duration (in minutes) for flies presented in C. A Two-tailed Mann-Whitney U test revealed that daytime sleep bout duration is increased in *dFB-Split>Kir2.1* male flies. **P<0.01. n=69-75 flies per genotype.

F) Box plots of nighttime sleep bout duration (in minutes) for flies presented in C. A Two-tailed Mann-Whitney U test revealed that nighttime sleep bout duration is increased in *dFB-Split>Kir2.1* male flies. ***P<0.001. n=69-75 flies per genotype.

The raw data underlying parts B, C, D, E, and F can be found in S1 Data.

S14 Fig. Courtship indices for untrained and trained flies.

A) Courtship index values for male flies in untrained and trained groups for each condition presented in Fig 5C. Unpaired parametric t-test for each group of untrained and trained males for each condition. Sample size (untrained:trained) from left to right on the graph, n = 54 (27:27), 51 (27:24), 49 (27:22), 51 (26:25), 46 (21:25), and 53 (27:26), respectively. Courtship indices < 10% were excluded from both groups. **P< 0.01, ns= not significant.

The raw data underlying part A can be found in S1 Data.

S1 Table: Description of FBS lines.

Identification of the AD construct combined with 23E10-DBD in each FBS line. Average number ± SEM and range of dFB neurons labeled by each line. Bowtie-VNC-SP (Y/N) indicates whether "bowtie" processes are seen in the brain and VNC-SP cell bodies are present in the VNC, Y= yes, N= no. Range of additional (non-dFB) neurons labeled in the brain of each line. Average number ± SEM of VNC metathoracic cells labeled by each FBS line. TPN1 (Y/N) indicates whether TPN1 neurons are present in the expression pattern, Y= yes, N= no. Range of additional cells in the VNC include any VNC neurons that is not TPN1 or VNC-SP.

The raw data underlying S1 Table can be found in S1 Data.

S2 Table: Summary of sleep phenotypes obtained for thermogenetic and optogenetic activation of FBS lines.

S3 Table: List of fly stocks used in this study.

S1 Movie. Brain of a dFB-Split>UAS-GFP female.

S2 Movie. VNC of a dFB-Split>UAS-GFP female.

S3 Movie. Brain of a 84C10AD; ChAT-DBD>UAS-GFP female.

S4 Movie. VNC of a 84C10AD; ChAT-DBD>UAS-GFP female.

S5 Movie. Brain of a VGlut-AD; 84C10-DBD>UAS-GFP female.

S6 Movie. VNC of a VGlut-AD; 84C10-DBD>UAS-GFP female.

S1 Data: Raw data underlying all Figs.

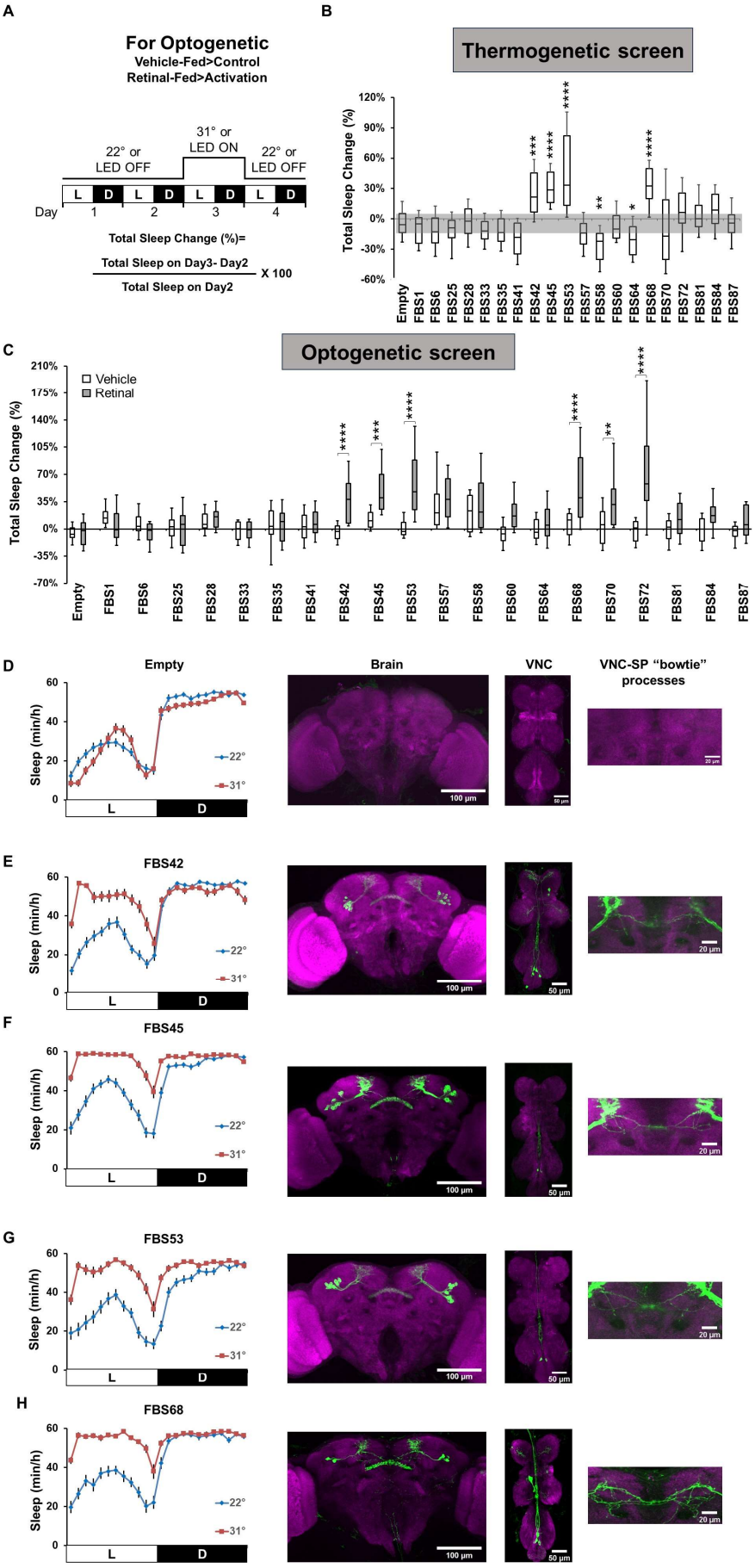
A
For Optogenetic
Vehicle-Fed>Control
Retinal-Fed>Activation
22° or LED OFF
31° or LED ON
22° or LED OFF
L D L D L D L D
Day 1 2 3 4
Total Sleep Change (%)=
Total Sleep on Day3- Day2
Total Sleep on Day2
X 100
B
Thermogenetic screen
Total Sleep Change (%)
120% 90% 60% 30% 0% -30% -60%
Empty FBS1 FBS6 FBS25 FBS28 FBS33 FBS35 FBS41 FBS42 FBS45 FBS53 FBS57 FBS58 FBS60 FBS64 FBS68 FBS70 FBS72 FBS81 FBS84 FBS87
C
Optogenetic screen
Vehicle
Retinal
Total Sleep Change (%)
210% 175% 140% 105% 70% 35% 0% -35% -70%
Empty FBS1 FBS6 FBS25 FBS28 FBS33 FBS35 FBS41 FBS42 FBS45 FBS53 FBS57 FBS58 FBS60 FBS64 FBS68 FBS70 FBS72 FBS81 FBS84 FBS87
D
Empty
Brain
VNC
VNC-SP "bowtie" processes
Sleep (min/h)
22°
31°
L D
100 µm
50 µm
20 µm
E
FBS42
F
FBS45
G
FBS53
H
FBS68

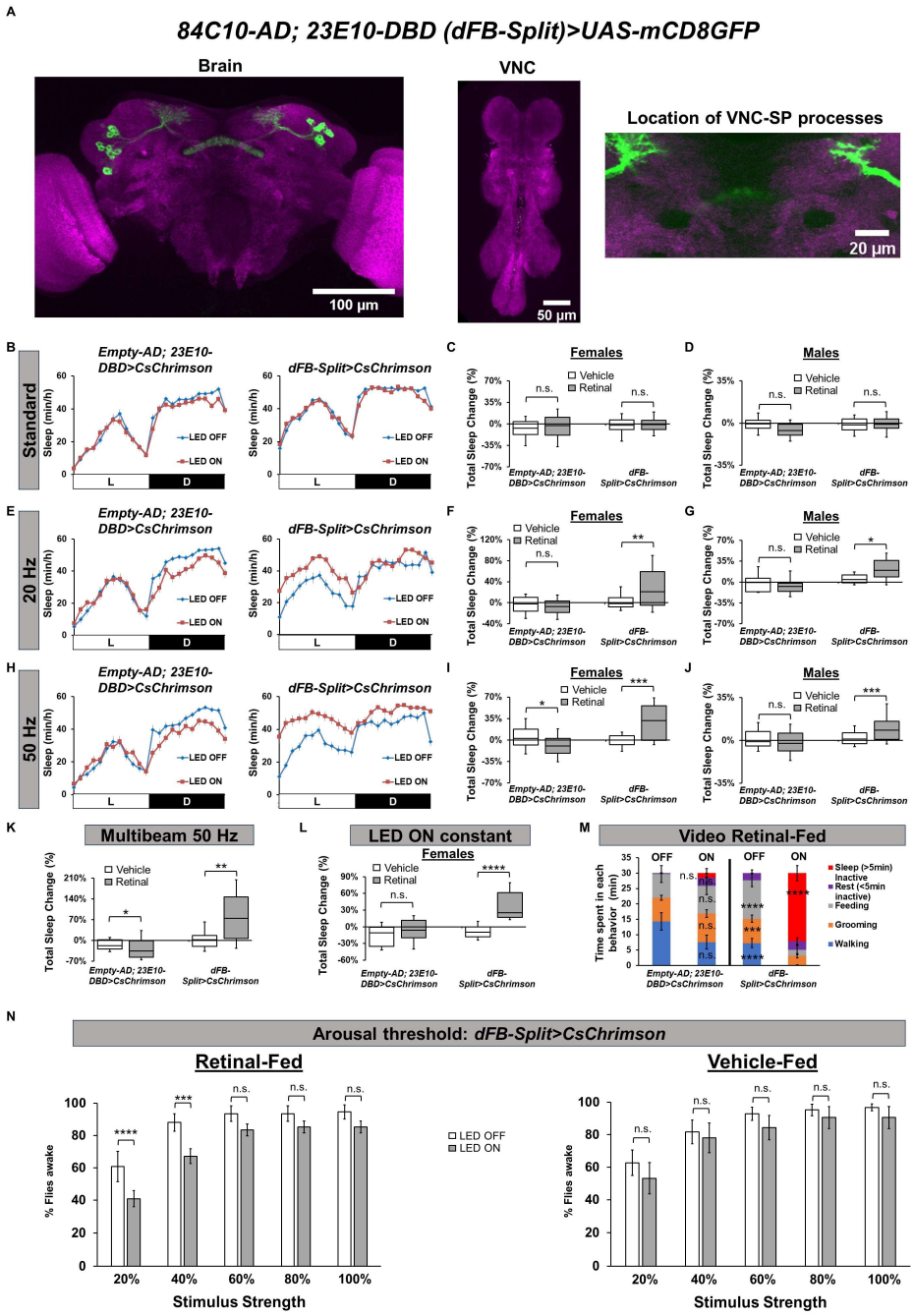
A
84C10-AD; 23E10-DBD (dFB-Split)>UAS-mCD8GFP
Brain
100 µm
VNC
50 µm
Location of VNC-SP processes
20 µm
B
Standard
Empty-AD; 23E10-DBD>CsChrimson
dFB-Split>CsChrimson
Sleep (min/h)
LED OFF
LED ON
L
D
C
Females
D
Males
Vehicle
Retinal
Total Sleep Change (%)
n.s.
E
20 Hz
F
G
H
50 Hz
I
J
K
Multibeam 50 Hz
L
LED ON constant
M
Video Retinal-Fed
OFF
ON
Time spent in each behavior (min)
Sleep (>5min) Inactive
Rest (<5min inactive)
Feeding
Grooming
Walking
N
Arousal threshold: dFB-Split>CsChrimson
Retinal-Fed
Vehicle-Fed
% Flies awake
Stimulus Strength
20%
40%
60%
80%
100%

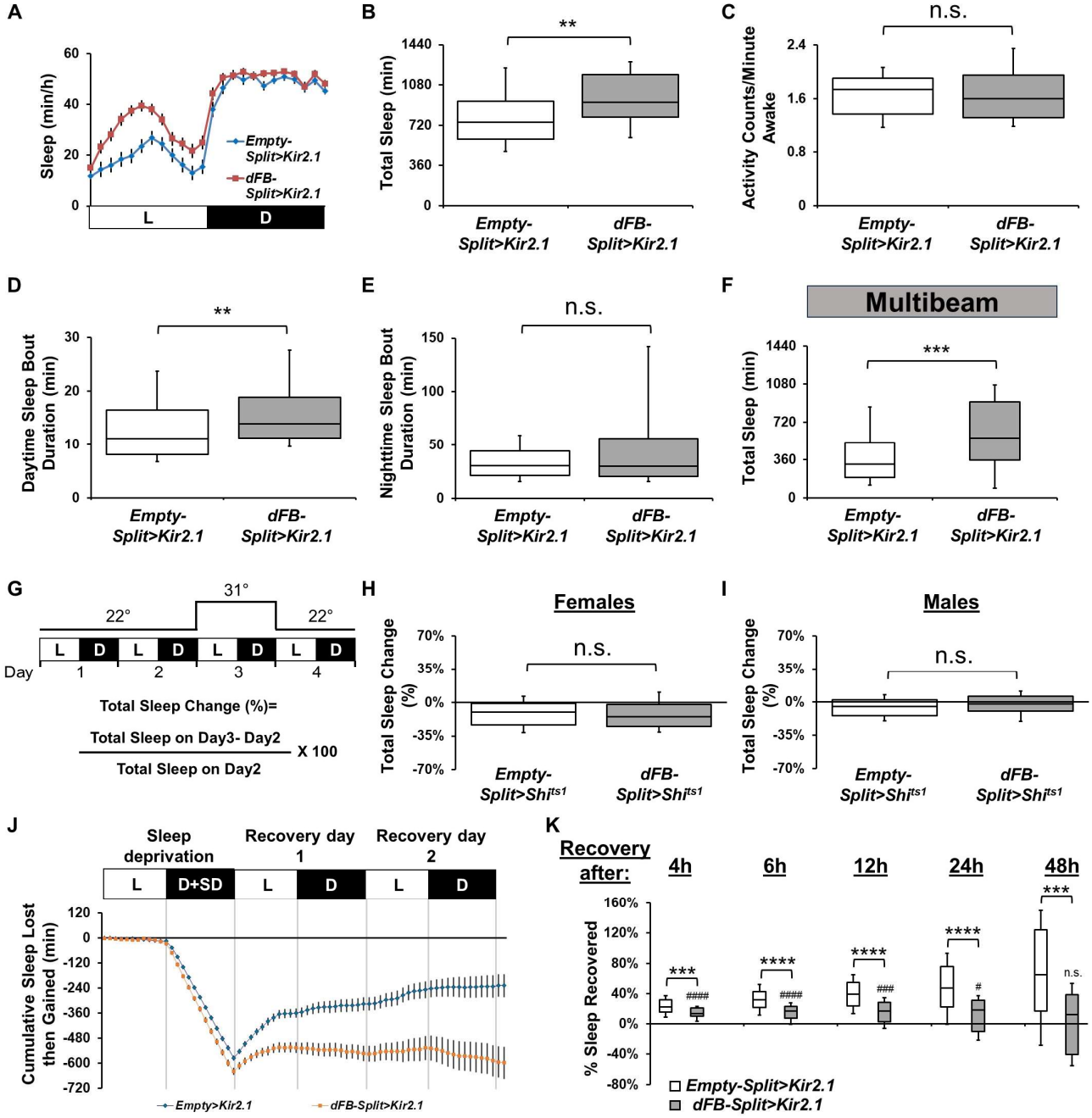
A
Sleep (min/h)
60
40
20
0
L
D
Empty-Split>Kir2.1
dFB-Split>Kir2.1
B
Total Sleep (min)
1440
1080
720
360
0
**
Empty-Split>Kir2.1
dFB-Split>Kir2.1
C
Activity Counts/Minute Awake
2.4
1.6
0.8
0
n.s.
Empty-Split>Kir2.1
dFB-Split>Kir2.1
D
Daytime Sleep Bout Duration (min)
30
20
10
0
**
Empty-Split>Kir2.1
dFB-Split>Kir2.1
E
Nighttime Sleep Bout Duration (min)
150
100
50
0
n.s.
Empty-Split>Kir2.1
dFB-Split>Kir2.1
F
Multibeam
Total Sleep (min)
1440
1080
720
360
0
***
Empty-Split>Kir2.1
dFB-Split>Kir2.1
G
22°
31°
22°
L D L D L D L D
Day 1 2 3 4
Total Sleep Change (%)=
Total Sleep on Day3- Day2
Total Sleep on Day2
X 100
H
Females
Total Sleep Change (%)
70%
35%
0%
-35%
-70%
n.s.
Empty-Split>Shi^ts1
dFB-Split>Shi^ts1
I
Males
Total Sleep Change (%)
70%
35%
0%
-35%
-70%
n.s.
Empty-Split>Shi^ts1
dFB-Split>Shi^ts1
J
Sleep deprivation
Recovery day 1
Recovery day 2
L
D+SD
L
D
L
D
Cumulative Sleep Lost then Gained (min)
120
0
-120
-240
-360
-480
-600
-720
Empty>Kir2.1
dFB-Split>Kir2.1
K
Recovery after:
4h
6h
12h
24h
48h
% Sleep Recovered
160%
120%
80%
40%
0%
-40%
-80%
***
####
****
####
****
###
****
#
***
n.s.
Empty-Split>Kir2.1
dFB-Split>Kir2.1

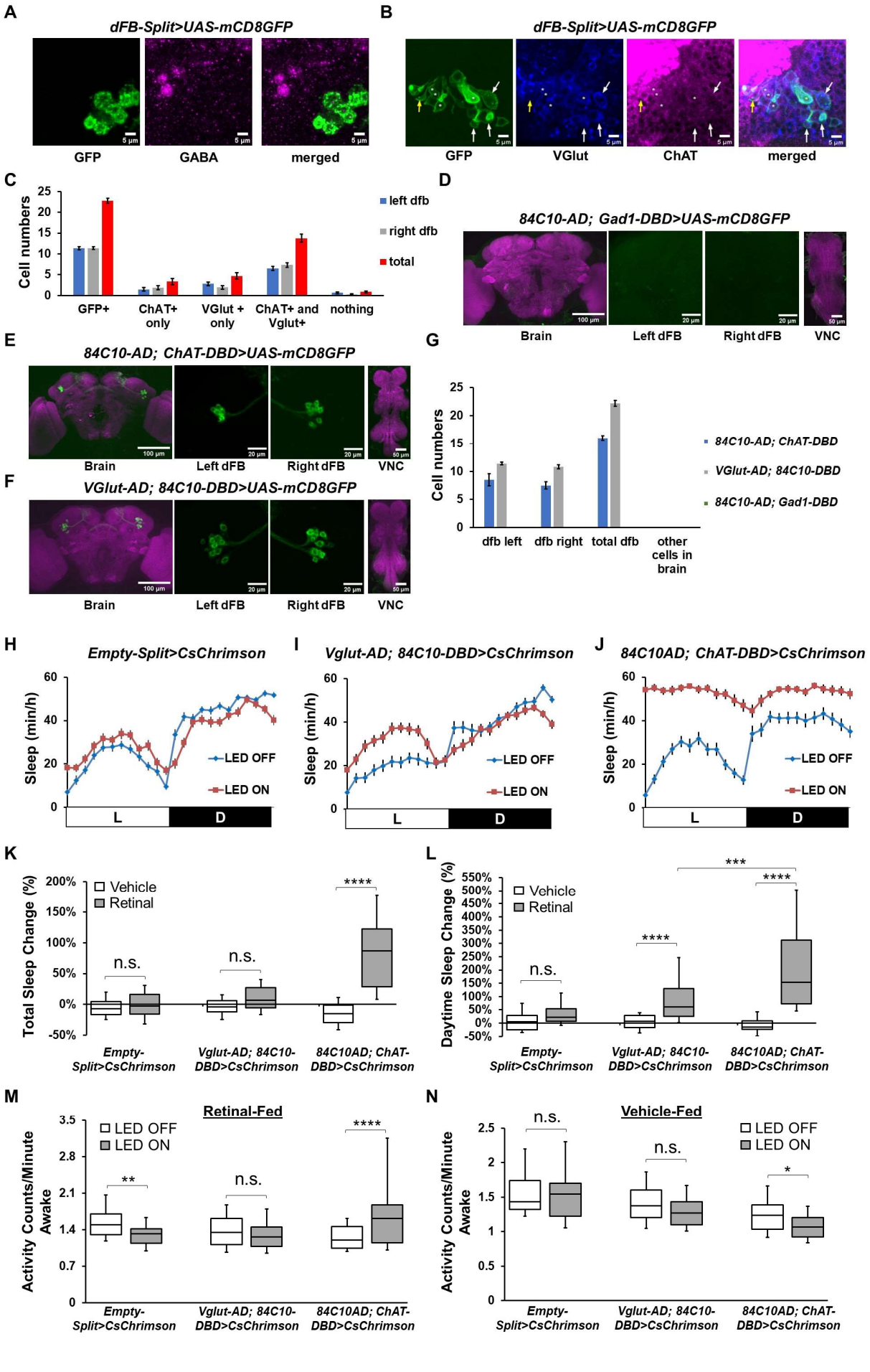
A
dFB-Split>UAS-mCD8GFP
GFP
GABA
merged
B
dFB-Split>UAS-mCD8GFP
GFP
VGlut
ChAT
merged
C
Cell numbers
left dfb
right dfb
total
GFP+
ChAT+ only
VGlut + only
ChAT+ and Vglut+
nothing
D
84C10-AD; Gad1-DBD>UAS-mCD8GFP
Brain
Left dFB
Right dFB
VNC
E
84C10-AD; ChAT-DBD>UAS-mCD8GFP
Brain
Left dFB
Right dFB
VNC
F
VGlut-AD; 84C10-DBD>UAS-mCD8GFP
Brain
Left dFB
Right dFB
VNC
G
Cell numbers
84C10-AD; ChAT-DBD
VGlut-AD; 84C10-DBD
84C10-AD; Gad1-DBD
dfb left
dfb right
total dfb
other cells in brain
H
Empty-Split>CsChrimson
Sleep (min/h)
LED OFF
LED ON
L
D
I
Vglut-AD; 84C10-DBD>CsChrimson
Sleep (min/h)
LED OFF
LED ON
L
D
J
84C10AD; ChAT-DBD>CsChrimson
Sleep (min/h)
LED OFF
LED ON
L
D
K
Total Sleep Change (%)
Vehicle
Retinal
n.s.
n.s.
****
Empty-Split>CsChrimson
Vglut-AD; 84C10-DBD>CsChrimson
84C10AD; ChAT-DBD>CsChrimson
L
Daytime Sleep Change (%)
Vehicle
Retinal
n.s.
****
***
****
Empty-Split>CsChrimson
Vglut-AD; 84C10-DBD>CsChrimson
84C10AD; ChAT-DBD>CsChrimson
M
Retinal-Fed
Activity Counts/Minute Awake
LED OFF
LED ON
**
n.s.
****
Empty-Split>CsChrimson
Vglut-AD; 84C10-DBD>CsChrimson
84C10AD; ChAT-DBD>CsChrimson
N
Vehicle-Fed
Activity Counts/Minute Awake
n.s.
n.s.
*
LED OFF
LED ON
Empty-Split>CsChrimson
Vglut-AD; 84C10-DBD>CsChrimson
84C10AD; ChAT-DBD>CsChrimson

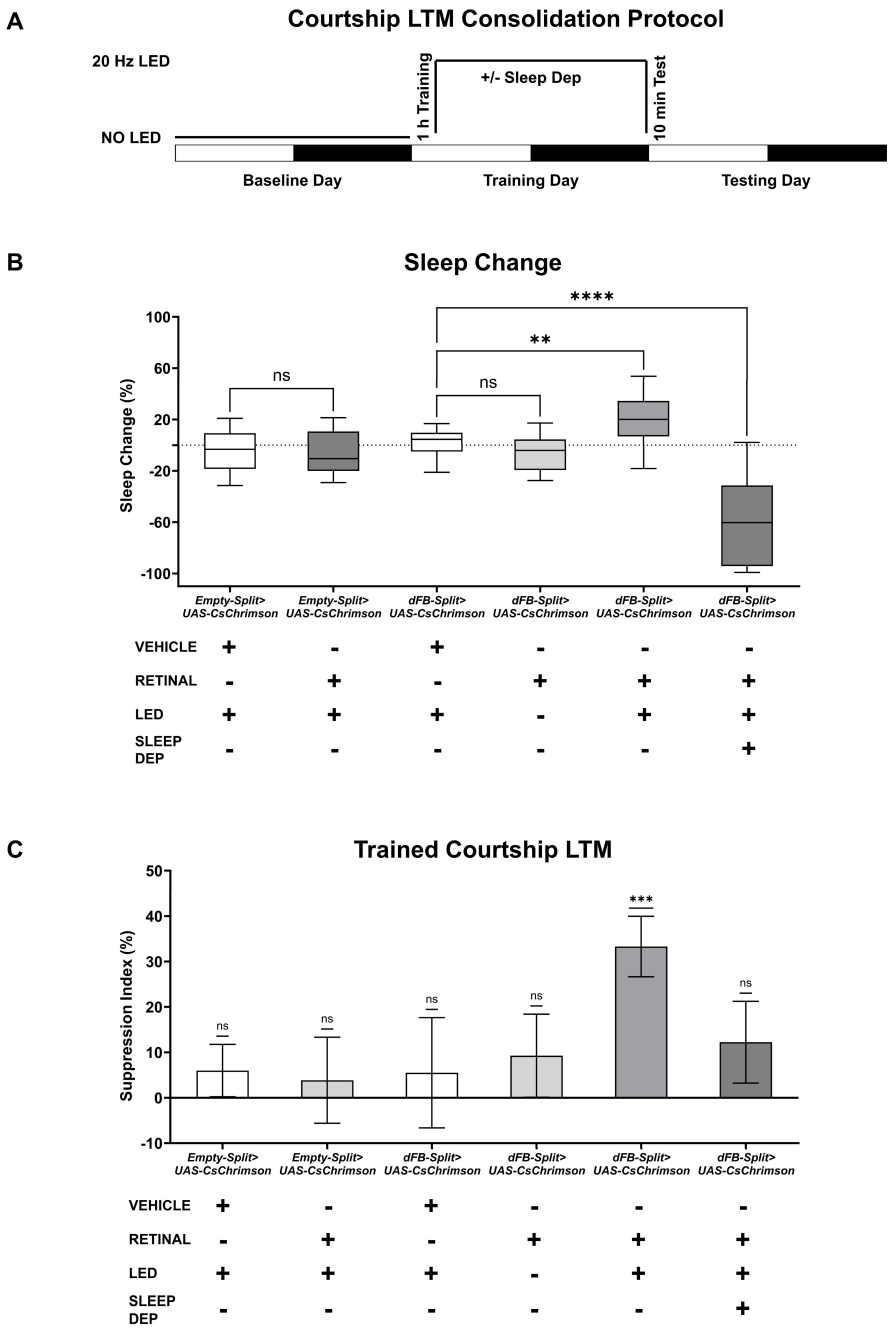
A
Courtship LTM Consolidation Protocol
20 Hz LED
NO LED
1 h Training
+/- Sleep Dep
10 min Test
Baseline Day
Training Day
Testing Day
B
Sleep Change
Sleep Change (%)
100
60
20
-20
-60
-100
ns
ns
**
****
Empty-Split> UAS-CsChrimson
Empty-Split> UAS-CsChrimson
dFB-Split> UAS-CsChrimson
dFB-Split> UAS-CsChrimson
dFB-Split> UAS-CsChrimson
dFB-Split> UAS-CsChrimson
VEHICLE + - + - - -
RETINAL - + - + + +
LED + + + - + +
SLEEP DEP - - - - - +
C
Trained Courtship LTM
Suppression Index (%)
50
40
30
20
10
0
-10
ns
ns
ns
ns
***
ns
Empty-Split> UAS-CsChrimson
Empty-Split> UAS-CsChrimson
dFB-Split> UAS-CsChrimson
dFB-Split> UAS-CsChrimson
dFB-Split> UAS-CsChrimson
dFB-Split> UAS-CsChrimson
VEHICLE + - + - - -
RETINAL - + - + + +
LED + + + - + +
SLEEP DEP - - - - - +